Master's Thesis in Chemical Engineering for Energy and Environment

Dynamic Reactor Modeling and Operational Optimization of Flexible E-Methanol Production

SEONGGYUN KIM

KTH ROYAL INSTITUTE OF TECHNOLOGY

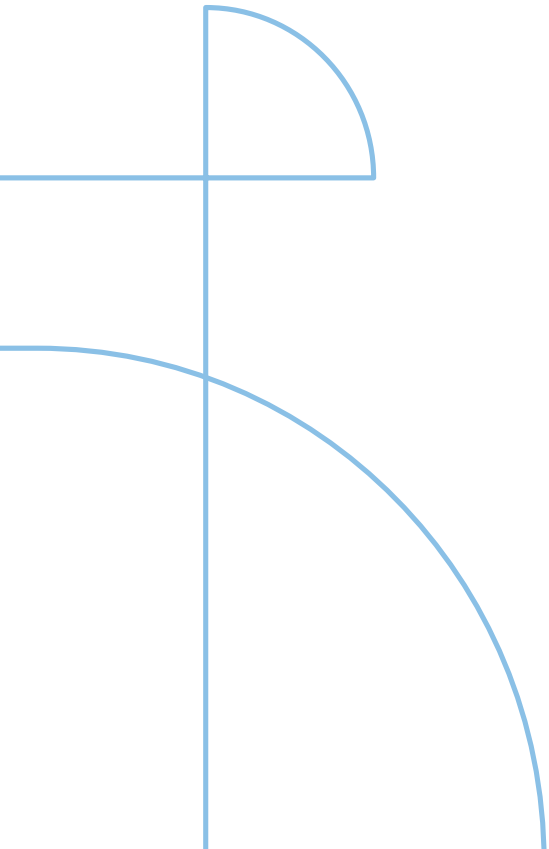

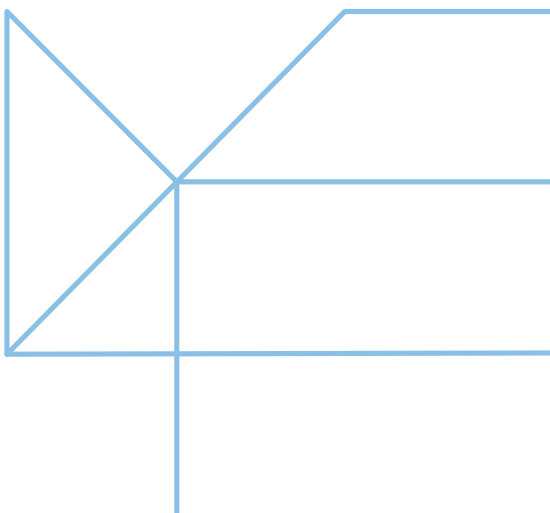

Dynamic Reactor Modeling and Operational Optimization of Flexible E-Methanol Production

Seonggyun Kim

Supervisors: Stefan Grönkvist, Kumail Marnate

Master's Thesis in Chemical Engineering for Energy and Environment

KTH Royal Institute of Technology

Stockholm, Sweden 2025

Abstract

This thesis investigates the economic viability of flexible e-methanol production in response to volatile electricity markets. The increasing penetration of renewable energy sources has led to significant electricity price volatility, creating opportunities for hydrogen production from electrolysis and conversion into various chemicals that can adapt their operational schedules to capitalize on favorable market conditions. E-methanol synthesis is a unique opportunity in power-to-chemicals pathways by simultaneously utilizing renewable electricity and captured CO_2 as feedstock.

However, methanol production involves high-temperature catalytic reactors with operational constraints that traditionally favor continuous operation. This study aims to quantify the economic benefits of flexible operation while accounting for technical challenges and operational costs of variable production.

This work integrates (i) a steady-state process model and a dynamic reactor model on Aspen Plus/Aspen Dynamics for verifying realistic flexibility limits (ramp rates, stabilization times, minimum load) with (ii) an optimization model based on mixed-integer linear programming (MILP) that embeds those constraints to optimize yearly operating schedules against historical Swedish electricity prices (2019–2023). This framework combines physical feasibility to economic performance, enabling a comprehensive assessment of flexible operation strategies.

Results demonstrate that flexible operation achieves production cost changes ranging from 0 to 441 EUR/tonne depending on market volatility, representing cost reductions of up to 24.5 % compared to constant-capacity operation. The economic benefits correlate strongly with electricity price volatility: stable market years (2019–2020) show modest cost changes of 0.2–8.6 EUR/tonne, while volatile years (2021–2023) enable substantial savings of 103.6–441 EUR/tonne. Optimal strategies adapt operational patterns to market conditions, operating at full capacity 47.5–99.0 % of the time. The analysis establishes that operational flexibility becomes economically essential during periods of high electricity price volatility, providing a cost mitigation strategy for industrial chemical production in increasingly volatile energy markets. Importantly, future power-to-X (PtX) system designs should treat flexibility characteristics (ramp rate, minimum load, response latency) as first-order design variables rather than downstream operational adjustments.

Sammanfattning

Denna avhandling undersöker den ekonomiska potentialen hos flexibel e-metanolproduktion i en volatil elmarknad. Den växande andelen förnybar el har lett till kraftigt varierande elpriser, vilket skapar möjligheter för processer som kan anpassa driften efter marknadsförhållandena. E-metanol erbjuder en särskilt intressant väg inom power-to-chemicals genom att kombinera förnybar el med infångad CO_2 som råvara.

Metanolproduktion bygger dock på högtemperatur-katalytiska reaktorer med tekniska begränsningar som normalt gynnar kontinuerlig drift. Studien syftar därför till att kvantifiera de ekonomiska fördelarna med flexibel drift, samtidigt som de tekniska utmaningarna och de driftmässiga kostnaderna vid varierande produktion beaktas.

Metodiken kombinerar en stationär processmodell med en dynamisk reaktormodell i Aspen Plus/Aspen Dynamics för att verifiera realistiska flexibilitetsgränser (rampningshastigheter, stabiliseringstider, minimallast). Dessa begränsningar integreras i en optimeringsmodell baserad på blandad heltalslinjärprogrammering (mixed-integer linear programming, MILP) som optimerar driftscheman baserat på historiska svenska elpriser (2019–2023). Detta ramverk kopplar samman fysisk genomförbarhet med ekonomisk prestanda, vilket möjliggör en omfattande utvärdering av flexibla driftstrategier.

Resultaten visar att flexibel drift uppnår produktionskostnadsförändringar från 0 till 441 EUR/ton beroende på marknadsvolatilitet, vilket motsvarar kostnadsminskningar på upp till 24,5 % jämfört med konstant kapacitet. De ekonomiska fördelarna korrelerar starkt med elprisvolatilitet: stabila marknadsår (2019–2020) visar blygsamma kostnadsförändringar på 0,2–8,6 EUR/ton, medan volatila år (2021–2023) möjliggör betydande besparingar på 103,6–441 EUR/ton. Optimala strategier anpassar driftmönster efter marknadsförhållanden, med drift vid full kapacitet 47,5–99,0 % av tiden. Analysen fastställer att driftflexibilitet blir ekonomiskt avgörande under perioder med hög elprisvolatilitet och utgör en kostnadsmildrande strategi för industriell kemikalieproduktion i allt mer volatila energimarknader. Framtida power-to-X-system bör därför behandla flexibilitetsegenskaper (rampningshastighet, minimallast, responstid) som primära designvariabler snarare än efterhandsanpassningar i driften.

List of Abbreviations

AACE	Association for the Advancement of Cost Engineering
APEA	Aspen Process Economic Analyzer
ASME	American Society of Mechanical Engineers
AWE	alkaline water electrolysis
CAPEX	capital expenditure
CHP	combined heat and power
EOS	equation of state
LCoM	levelized cost of methanol
LHHW	Langmuir-Hinshelwood-Hougen-Watson
LPMeOH	Liquid Phase Methanol
MILP	mixed-integer linear programming
NRTL	Non-Random Two-Liquid
OPEX	operating expenditure
PDE	partial differential equation
PEM	proton exchange membrane
PID	proportional-integral-derivative
PR	Peng-Robinson
PSRK	Predictive Soave-Redlich-Kwong
PtM	power-to-methanol
PtX	power-to-X
RMS	root-mean-square

Contents

1 Introduction

This chapter introduces the global energy transition context, the economic implications of electricity market dynamics, and the definition and importance of power-to-X (PtX) technologies. It establishes the motivation for studying flexible methanol production as a case study for demand-side flexibility in renewable energy systems, identifying the key technical and economic challenges that drive this research.

The Energy Storage Challenge and Power-to-X Solutions

The global transition toward renewable energy sources has fundamentally altered the electricity generation landscape. In 2023, a record 473 GW of renewable capacity was added globally, expanding the total stock by 13.9 % [1]. This brought the total share of renewables to 43 % of the world's installed power capacity [2]. By 2024, this trend continued, with total renewable capacity reaching approximately 4.4 TW [3]. Solar and wind power have been the primary drivers of this expansion, accounting for 98 % of all new renewable capacity in 2023 [1].

However, the inherent variability of these sources creates significant challenges for grid stability. Unlike dispatchable conventional power plants, renewable generation is subject to weather-dependent fluctuations, leading to unprecedented electricity price volatility [4, 5]. Electricity market volatility is further amplified by geopolitical risks beyond renewable variability itself [4, 6]. The 2022 energy crisis exemplified this, as the Russian full-scale invasion of Ukraine triggered unprecedented price volatility across European electricity markets [4]. Such geopolitical disruptions alter market fundamentals through supply chain disruptions, fuel commodity shocks, and emergency policy interventions, creating price dynamics that are inherently difficult to forecast using conventional market models [7].

This combined technical and geopolitical volatility creates an economic imperative for solutions that can balance supply and demand while managing price risk. Traditional grid balancing has relied on supply-side flexibility, but achieving the scale of renewable integration targeted in the European Green Deal [8] and national climate plans is widely expected to require complementary demand-side flexibility and long-duration energy storage [9]. Chemical energy carriers, produced via PtX pathways have emerged as a promising solution for this challenge, enabling both long-term storage and the coupling of the electricity sector with industries like shipping, aviation, and chemical manufacturing [10].

Burre et al. [10] define PtX processes as "processes with the goal to exploit the environmental and economic potential of renewable electricity". The economic viability of PtX is fundamentally linked to electricity costs; for PtX routes such as renewable methanol, electricity can account for up to 70 % of total production costs [11]. Increasing deployment of renewables may create opportunities for flexible industrial processes to reduce electricity costs by operating when prices are low.

Power-to-X Pathways

PtX processes are by nature hydrogen-centric: electricity is converted to H_2 via water electrolysis. However, direct hydrogen storage remains challenging due to its low volumetric energy density, requiring either high-pressure compression, cryogenic liquefaction, or conversion to chemical carriers. Consequently, H_2 is often converted into other chemicals—such as ammonia, methane, or methanol—that offer more practical storage and transport characteristics. Among the leading PtX pathways, ammonia (NH_3), synthetic methane (CH_4), and methanol (CH_3OH) each offer distinct technical and economic characteristics that influence their suitability for flexible operation and market integration.

Ammonia synthesis is a mature technology based on the Haber–Bosch process ($N_2 + 3\,H_2 \longrightarrow 2\,NH_3$), with a global production capacity of approximately 235 Mt in 2023 [12]. The push for decarbonization has created a substantial pipeline for low-emission ammonia, with 490 production plants in development by end of 2024 representing 438 Mt/y of low-emission and transitional ammonia capacity [13]. Ammonia has excellent energy density and hydrogen content [14], however, the decomposition ("cracking") back to H_2 is highly endothermic and imposes a significant efficiency penalty [15].

Synthetic methane production via the Sabatier process ($CO_2 + 4\,H_2 \longrightarrow CH_4 + 2\,H_2O$) is among the most technologically mature CO_2-utilizing PtX pathways, typically operated at 50–100 bar and 200–400 °C, with advanced plants reporting process efficiencies around 72 % [16]. A key advantage is infrastructure compatibility, leveraging the existing natural gas network, which represents approximately 3 trillion USD in asset value as of 2024 [17]. However, when considered as a hydrogen carrier, its storage and transport often require cryogenic liquefaction, and downstream H_2 recovery via reforming or pyrolysis is energy-intensive [18], similar to ammonia.

E-methanol synthesis via catalytic hydrogenation of captured CO_2 ($CO_2 + 3\,H_2 \longrightarrow CH_3OH + H_2O$) represents a promising pathway for renewable energy storage, with the global methanol market valued at 32.7 billion USD in 2024 [19].

This work focuses on power-to-methanol (PtM) because methanol offers unique advantages both as a PtX chemical product and as a hydrogen carrier. As a PtX process, methanol synthesis operates at moderate conditions (210–270 °C and 50–80 bar) that facilitate more responsive load changes. As a hydrogen carrier, methanol is liquid at ambient conditions, eliminating the pressurization or cryogenic storage requirements of ammonia and methane. More importantly, H_2 recovery via methanol steam reforming occurs under relatively mild conditions (200–350 °C), compared to the

significantly more demanding requirements of ammonia cracking (500–650 °C) or methane steam reforming (700–950 °C, 20–30 bar) [20]. These operational advantages make methanol particularly well-suited for price-responsive, dynamically operated PtX plants.

The Flexibility Challenge in PtX

In general, industrial processes can show a wide spectrum of flexibility. Electrochemical processes like water electrolysis are exceptionally flexible; modern electrolyzers such as alkaline water electrolysis (AWE) and proton exchange membrane (PEM) can operate across a load range of 0–100 % of nominal capacity and achieve ramp rates as high as 10 % of nominal capacity per second [21].

In contrast, thermochemical processes involving heterogeneous catalysis and significant thermal mass are typically less flexible—conventionally, these processes operate at steady-state full load, with the alternative being turndown to a load above the minimum load (20–40 %) rather than continuous or dynamic modulation. Recent studies reveal that the flexibility of methanol synthesis reactors is defined by thermal management challenges, catalyst performance limits, and process integration complexities [22–25]. This effectively makes the methanol synthesis process the flexibility bottleneck in the entire PtM chain, representing the main flexibility challenge.

2 Background

This chapter reviews the current state of research on PtM systems and identifies the specific technical gaps that motivate this work. The focus is on reactor-level dynamics and process integration challenges that ultimately determine the feasibility of flexible e-methanol production under variable renewable energy input.

2.1 Literature Review

Reactor Dynamics and Control

Recent advances in methanol reactor modeling have established the technical foundation for understanding flexibility constraints. Rinaldi and Visconti [26] demonstrated that multi-tubular reactors can transition between different operating modes and reach steady-state conditions within a few hours, proposing operational strategies where CO_2 utilization varies with renewable hydrogen availability. Nguyen [27] quantified achievable performance under 50 %/h ramp rates with 18.8 % minimum load, while Mbatha et al. [22] showed that appropriately designed reactors can achieve ramp rates up to 16.7 %/min and operate down to 20 % load.

The thermal management challenge represents a critical constraint in reactor flexibility. Rinaldi and Visconti [26] identified that reactor design significantly affects thermal gradients during transient operation, demonstrating that reducing tube numbers rather than tube length provides better thermal management. Montebelli et al. [28] showed that advanced heat transfer designs using monolith and foam catalysts can improve thermal response under dynamic conditions.

Control Strategy

Control system development has focused on managing the complex interactions during load changes. Nguyen et al. [23] introduced cascade proportional-integral-derivative (PID) controllers and lag filters for flow ramping, while Cui et al. [24] developed hybrid approaches combining detailed simulation with surrogate models for computational efficiency during dynamic optimization.

Process Integration and System-Level Constraints

Sivert [29] and Mucci et al. [30] identified methanol reactors as the primary bottleneck in flexible operation, confirming that within the methanol synthesis process, system-wide flexibility is constrained by the reactor rather than other unit operations such as compressors, heat exchangers, or separation equipment. This finding justifies focusing research efforts on reactor-level constraints as the key limitation for flexible methanol production.

Despite significant progress in dynamic modeling and control, several fundamental gaps limit the practical implementation of flexible e-methanol systems. Most existing studies examine either technical flexibility or economic optimization in isolation. Dynamic modeling studies [22, 26, 27] establish technical capabilities but rarely extend to economic evaluation under realistic market conditions. Conversely, economic optimization studies typically assume simplified constraints that may not reflect achievable reactor performance. This disconnect prevents quantitative assessment of the trade-offs between technical feasibility and economic viability.

Many flexibility studies implement idealized ramping profiles that may not reflect industrial-scale operational realities. Critical factors such as catalyst thermal stress limits, product quality maintenance during transients, and the interaction between multiple process units during load changes are often oversimplified, creating uncertainty about the practical achievability of predicted flexibility benefits. These simplifications represent typical challenges across all process modeling studies and remain present in this work as well.

2.2 Thesis Scope and Objectives

The identified research gaps motivate the development of an integrated modeling and optimization framework that bridges technical feasibility with economic viability. This thesis addresses these gaps through four specific objectives:

1. **Establish realistic operational boundaries** through detailed steady-state and dynamic process modeling in Aspen Plus and Aspen Plus Dynamics, quantifying achievable ramping rates, minimum load requirements, and stabilization times that reflect industrial-scale operational realities.
2. **Develop integrated dynamic-economic models** that combine detailed process constraints with mixed-integer linear programming optimization to evaluate flexible operation strategies under realistic electricity market conditions.
3. **Conduct a comprehensive multi-year economic assessment** using historical electricity price data to quantify the economic benefits of flexible operation and identify key sensitivity parameters affecting long-term profitability.
4. **Quantify design and operational trade-offs** between capital costs, operational flexibility,

and economic performance to provide decision-making guidance for industrial implementation.

By integrating detailed process modeling with comprehensive economic optimization, this work provides a comprehensive framework for evaluating the practical potential of flexible e-methanol production as a pathway for renewable energy integration and sustainable chemical synthesis. The methodology, described in the following chapter, combines engineering rigor with economic realism to ensure that findings reflect achievable performance rather than theoretical ideals.

3 Methods

The methodology follows a staged approach, as illustrated in figure 3.1. First, a complete e-methanol synthesis process is modeled at design capacity in Aspen Plus V14, based on the hydrogenation of pure CO_2 with H_2 produced via water electrolysis. The catalytic reactor model is then exported to Aspen Plus Dynamics to evaluate its transient response to time-varying inlet flowrates. This dynamic simulation supports the validation of ramping behavior and the assessment of reactor flexibility. In the final stage, equipment sizing, capital costs, and operating expenses obtained from the simulations are incorporated into a mixed-integer linear programming (MILP) optimization. Additional techno-economic inputs, including electrolyzer costs, captured CO_2 pricing, and historical hourly electricity prices, are also integrated. The optimization focuses on key constraints in flexible operation, particularly those associated with the reactor, and compares the economic and operational performance of dynamic versus steady-state operation.

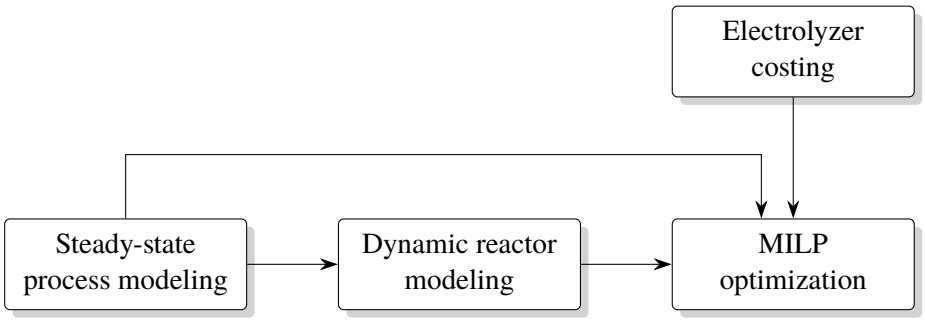

Figure 3.1: Comprehensive methodology overview for e-methanol plant optimization study.

3.1 Steady-State Process Modeling

A complete steady-state process model of methanol synthesis is developed in Aspen Plus V14. The purpose of the model is to evaluate key metrics for unit operations that serve as a basis for sizing and costing of the equipment in section 3.3.3 and to configure a reactor model to test and analyze in Aspen Plus Dynamics in section 3.2. This section outlines the main assumptions, process variables, and specifications applied in the model.

3.1.1 Thermodynamic and Kinetic Models

The selection of accurate numerical models for the chemical systems is a foundational step to building a robust process model. Detailed information on the selection of the thermodynamic model as well as the kinetics implementation procedure are presented in this section.

Thermodynamics

The thermodynamic model selection is critical for accurate prediction of phase equilibria, enthalpies, and fugacities of material streams present in the process. equations of state (EOSs) relate pressure, temperature, and composition to other thermodynamic properties and are particularly important for high-pressure gas-phase calculations. Activity coefficient models, on the other hand, are used to describe liquid-phase non-idealities and are more suitable for low-pressure vapor-liquid equilibrium calculations.

In the literature, the Predictive Soave-Redlich-Kwong (PSRK) and Non-Random Two-Liquid (NRTL) pair is commonly adopted for high- and low-pressure sections respectively [24, 27]. However, this work adopts Peng-Robinson (PR) EOS and NRTL pair for better convergence and to utilize pre-calibrated binary interaction parameters. This choice is supported by consultation with AspenTech customer support and is more consistent with Carlson's guideline for selecting thermophysical property models [31]. The PR EOS is used for all gas-phase unit operations, including compressors, heat exchangers, the reactor, and the high-pressure flash vessel. The NRTL model is applied in the low-pressure flash vessel and the distillation column to better capture non-idealities in the liquid phase.

Reaction Kinetics

Three chemical reactions, given in equations 3.1 to 3.3, are considered for methanol synthesis. Only two independent rate laws are implemented, as the third reaction can be expressed as a linear combination of the other two. The CO_2 hydrogenation reaction (equation 3.1) and the reverse water–gas shift reaction (equation 3.3) are modeled using kinetic parameters reported by Cui et al. [24].

$$CO_2 + 3\,H_2 \rightleftharpoons CH_3OH + H_2O \tag{3.1}$$

$$CO + 2\,H_2 \rightleftharpoons CH_3OH \tag{3.2}$$

$$CO_2 + H_2 \rightleftharpoons CO + H_2O \tag{3.3}$$

Vanden Bussche and Froment's kinetic model is employed [32], as it shows the best accuracy in the operating range of modern methanol synthesis reactors [33]. Since Aspen Plus only accepts custom

kinetic models in exponential form, an algebraic rearrangement of the original model is required. The rate expressions for methanol synthesis and the reverse water–gas shift in this form are given in equations 3.4 and 3.5 [24].

$$r_{CH_3OH} = \frac{k_1 P_{CO_2} P_{H_2} \left(1 - \frac{1}{K_{eq1}} \frac{P_{H_2O} P_{CH_3OH}}{P_{H_2}^3 P_{CO_2}}\right)}{\left(1 + k_2 \frac{P_{H_2O}}{P_{H_2}} + k_3 P_{H_2}^{0.5} + k_4 P_{H_2O}\right)^3} \tag{3.4}$$

$$r_{RWGS} = \frac{k_5 P_{CO_2} \left(1 - K_{eq2} \frac{P_{H_2O} P_{CO}}{P_{CO_2} P_{H_2}}\right)}{\left(1 + k_2 \frac{P_{H_2O}}{P_{H_2}} + k_3 P_{H_2}^{0.5} + k_4 P_{H_2O}\right)} \tag{3.5}$$

where: r_{CH_3OH}, r_{RWGS} = reaction rates for methanol synthesis and reverse water–gas shift
P_i = partial pressure of component i
$k_1, \ldots, k_5$ = kinetic rate constants
K_{eq1}, K_{eq2} = equilibrium constants for methanol synthesis and RWGS reactions

The kinetic parameters and equilibrium constants are given in equations 3.6 to 3.8 and table 3.1 [32].

$$k_i = A_i \exp \frac{B_i}{RT} \tag{3.6}$$

$$\log_{10} K_{eq1} = \frac{3066}{T} - 10.592 \tag{3.7}$$

$$\log_{10} \frac{1}{K_{eq2}} = -\frac{2073}{T} + 2.029 \tag{3.8}$$

where: A_i, B_i = pre-exponential factor and activation energy for rate constant k_i
R = universal gas constant
T = temperature

The kinetic parameters obtained after mapping them to Langmuir-Hinshelwood-Hougen-Watson (LHHW) rate expression are presented in table 3.2. The pre-exponential factors and temperature exponents are set as 1 and 0, respectively, since the expression of the driving force term includes the pre-exponential term as well as the temperature dependency in the rearranged equation. The adsorption terms reported by Vanden Bussche and Froment [32] are used without any conversion.

Model Validation

The thermodynamic and kinetic models are validated by comparing the simulation results with reference data reported by Vanden Bussche and Froment [32]. An `RPlug` reactor block is set up to

Table 3.1: Kinetic parameters in Vanden Bussche and Froment model [B in J/mol] [32].

Parameter	Constant	Value
k_1	A_1	1.97
	B_1	40 000
k_2	A_2	3 453.38
	B_2	–
k_3	A_3	0.499
	B_3	17 197
K_{CO_2}	A_4	6.62×10^{-11}
	B_4	124 119
K_{H_2O}	A_5	1.22×10^{10}
	B_5	−98 084

Table 3.2: Coefficients for driving force constants in the kinetic model.

Reaction	Parameter	CO_2 Hydrogenation	RWGS
Forward	A	−29.87	4.804
	B	4 811.2	−11 797.5
Backward	A	17.55	0.131
	B	−2 249.8	−7 023.5

match the bench-scale reactor conditions reported in [32], with specifications listed in table 3.3. The original plot in [32] is digitized using WebPlotDigitizer [34] to extract the data points for comparison. The validation results are presented in figure 3.2, showing good agreement between the model predictions and experimental data across all major components.

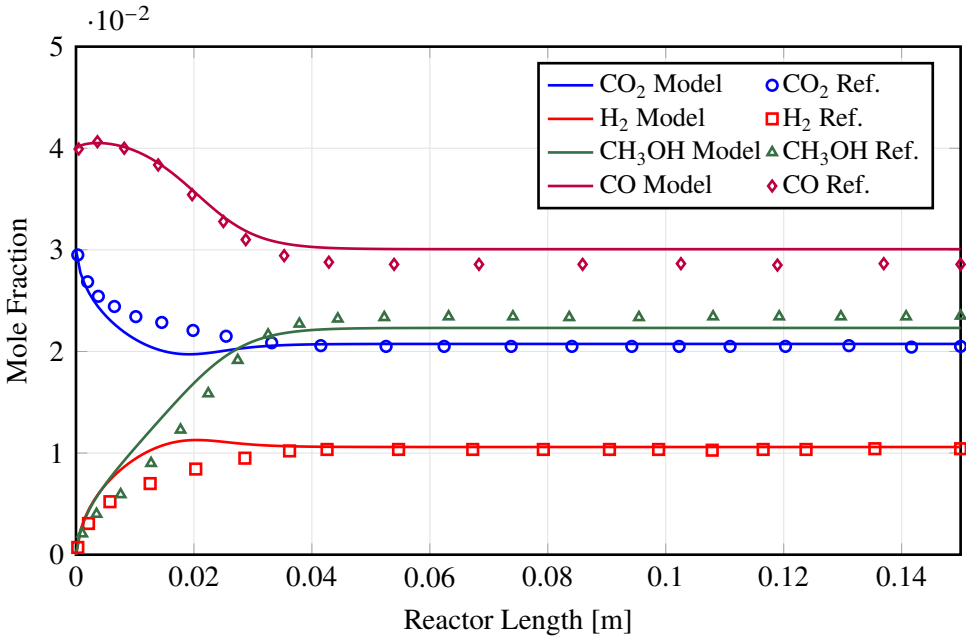

Figure 3.2: Kinetic model validation results.

Table 3.3: Validation reactor specifications [32].

Parameter	Value	Unit
Catalyst properties		
Density	1 775	kg/m³
Porosity	0.5	–
Pellet diameter	0.5	mm
Reactor geometry		
Diameter	0.016	m
Length	0.15	m
Operating conditions		
Temperature	493.2	K
Pressure	50	bar
Feed composition		
CO	4.00	mol%
H_2O	0.00	mol%
CH_3OH	0.00	mol%
H_2	82.00	mol%
CO_2	3.00	mol%
Ar	11.0	mol%

3.1.2 Process Description

With the thermophysical property model selected and kinetic reaction laws implemented, a complete methanol synthesis process is designed in Aspen Plus. The process capacity is set to CO_2 and H_2 flowrates of 100 kmol/h and 300 kmol/h, respectively, corresponding to a methanol production rate of about 27.8 kt/y and an electrolyzer capacity of 31.4 MW, based on a specific energy consumption of 52 kW h/kg H_2 [35].

Overall Scheme

The process consists of feed and recycle compressors, high- and low-pressure flash separation vessels, a CO_2 hydrogenation reactor, and a distillation column. It is assumed that pure CO_2 from a carbon capture process and H_2 from AWE enter the system. Figure 3.3 presents the overall flowsheet for the e-methanol synthesis process.

The feed of CO_2 and H_2 are compressed by compressors (K-1 and MK-1) and preheated by the feed-effluent heat exchanger (HX-1) before entering the catalytic multi-tubular reactor (R-1), a so-called "Lurgi-type" reactor. The outlet stream from the reactor passes two heat exchangers (HX-1 and HX-2) for heat recovery, then enters the high-pressure vessel (FV-1).

Unreacted gas separated from FV-1 is recompressed by a compressor (K-2) and fed back to the reactor, with 0.5 % purged to prevent accumulation of impurities. A vapor stream separated from the low-pressure vessel (FV-2) is purged, while the liquid stream is further purified in the distillation

column (D-1). The designed process achieves a methanol purity of 99.85 %, which satisfies the minimum purity requirements for commercial applications [36].

Specifications

A catalytic packed-bed plug flow reactor block (`RPlug`) and a rigorous distillation column block (`RadFrac`) are used for the reactor and the distillation column. `RPlug` is Aspen Plus's most configurable plug flow reactor model, capable of simulating reactions using user-defined kinetic expressions with heat transfer to or from a cooling medium. `RadFrac` is similarly the most rigorous column model, performing stage-by-stage vapor–liquid equilibrium calculations with options for reaction, heat integration, and rating. Compressors and heat exchangers are included to maintain constant reactor inlet conditions at 70 bar and 225 °C, and flash vessels operate at 69.4 bar and 1.1 bar. The reactor inlet conditions are chosen based on typical industrial operating ranges reported in the literature [24, 27, 37, 38] and summarized in table 3.4. The reactor is configured with a constant thermal fluid temperature on the shell side, representing boiling water cooling; the generated steam is used to supply heat to the reboiler. Table 3.5 summarizes all input specifications for the unit operation blocks.

The key operating conditions, such as reactor inlet pressure and temperature, are chosen based on typical ranges reported in the literature on CO_2-to-methanol synthesis simulation. Table 3.4 summarizes reactor inlet conditions from selected studies, confirming that the chosen parameters align with established practice.

Table 3.4: Comparison of reactor inlet conditions for CO_2-to-methanol synthesis from the literature.

Reference	T_{in} **(°C)**	P_{in} **(bar)**
Mbatha et al. [22]	240	75.7
Cui et al. [24]	220	31
Rinaldi and Visconti [26]	200	92.8
Bisotti et al. [37]	225	69.7
Chen et al. [38]	225	69.7
This work	220	70

3.2 Dynamic Reactor Modeling and Ramp Analysis

Following the steady-state process model, dynamic simulations are performed to assess the reactor's behavior under transient conditions. The main goal is to determine whether the process can be ramped between nominal and minimum loads and stabilize within one hour of the ramp. This one-hour criterion reflects the temporal resolution of electricity prices in the spot market: if the reactor can switch to a different load level and stabilize within one hour, then from the second hour onwards, the plant can fully exploit sustained price advantage that may persist over multiple hours.

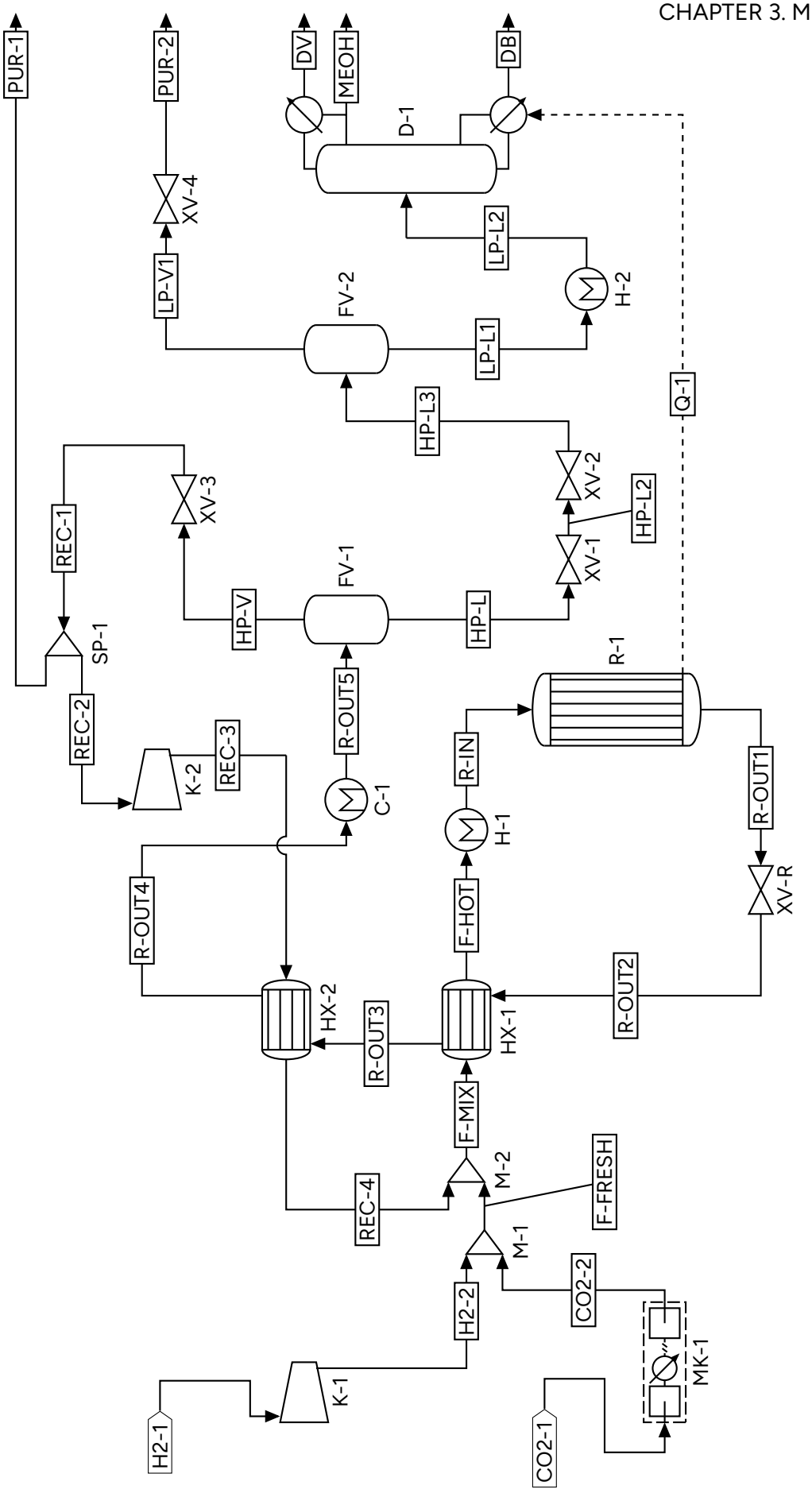

Figure 3.3: Methanol synthesis process flowsheet.

Table 3.5: Aspen Plus input specifications for the MeOH process.

Block	Specification	Value	Unit
Compressors[a]			
MK-1 (`MCompr`)	Discharge pressure	71	bar
	Number of stages	4	
K-1 (`Compr`)	Discharge pressure	71	bar
K-2 (`Compr`)	Discharge pressure	71	bar
Heat exchangers			
HX-1 (`HeatX`)	Hot stream outlet temp.	150	°C
HX-2 (`HeatX`)	Cold stream outlet temp.	120	°C
H-1 (`Heater`)	Outlet temperature	220	°C
	Pressure drop	0.5	bar
C-1 (`Heater`)	Outlet temperature	35	°C
	Pressure drop	0.5	bar
Reactor			
R-1 (`RPlug`)	Coolant temperature	220	°C
	Number of tubes	1817	
	Length	6	m
	Tube diameter	0.04	m
	Pressure drop correlation	Ergun	
	Catalyst bed voidage	0.4	
	Catalyst particle density	1775	kg/m³
	Catalyst particle diameter	5.4	mm
Flash vessels[b]			
FV-1 (`Flash2`)	Pressure	69.4	bar
FV-2 (`Flash2`)	Pressure	1.1	bar
Distillation column			
D-1 (`RadFrac`)	Condenser type	Partial	
	Number of stages	40	
	Condenser pressure	1.0	bar
	Reboiler duty[c]	1.58	MW
	Bottoms rate	101	kmol/hr

[a] The isentropic efficiency is 0.75 and the mechanical efficiency is 0.90 for all compressors.
[b] The duties are zero (adiabatic) for all flash vessels.
[c] Heat is supplied as steam generated from reactor cooling (heat stream Q-1 in figure 3.3).

Perfect price foresight is assumed throughout the optimization: the operator knows the full day-ahead prices before committing to operational decisions, so sustained price advantages can be identified in advance.

This section first outlines the scope and simplifying assumptions used to make the dynamic analysis tractable, then describes the ramping strategy implemented in Aspen Plus Dynamics. Subsequent subsections address the treatment of energy balance in the reactor model, the determination of minimum load and maximum ramp rates, and the method used for steady-state detection. Together, these elements define the operability constraints of the process and establish the basis for evaluating flexibility.

3.2.1 Model Scope and Assumptions

Introducing a time dimension to the steady-state model increases complexity, computational demand, and numerical challenges associated with solving a system of partial differential equations (PDEs). To maintain tractability, the dynamic analysis in this work is constrained by assumptions and simplifications designed to reduce the degrees of freedom while preserving the key insights of interest.

One of the key simplifications made in this work is to focus the dynamic analysis exclusively on the reactor model, rather than simulating the entire process. This approach is justified by the fact that the reactor is widely recognized as the primary bottleneck in flexible operation of methanol synthesis plants [30]. Other unit operations such as compressors, heat exchangers, and flash vessels are assumed to respond instantaneously to changes in flowrate and composition, given their relatively fast dynamics compared to the reactor. This assumption allows the dynamic simulation to isolate the reactor's transient behavior without the added complexity of other process elements, which while having their own operational challenges (such as compressor surge under dynamic operation), can be managed by engineering solutions like implementing anti-surge drums with valves that dampen the process fluctuations [22, 39].

However, this simplification comes with a limitation that the dynamic analysis cannot account for the interactions between the reactor and other unit operations. Especially, without a closed recycle loop, the recycled inlet stream cannot be calculated endogenously from other unit operations and must be specified externally. To address this limitation, both fresh and recycled feeds are manually ramped in parallel. Testing confirmed that this simplified approach yields results virtually identical to full recycle calculations, which is consistent with the short reactor residence time (on the order of seconds). The recycle stream's temperature, pressure, and composition are therefore taken directly from the steady-state model and held constant throughout the dynamic simulation. While in reality the temperature and composition of the recycle stream would vary slightly during transients, this assumption is reasonable given the small magnitude of these changes relative to the overall process conditions.

The ramping behavior of the inlet streams is implemented using the TASK function in Aspen Plus Dynamics, which provides precise control over time-dependent process variables through programmable specifications. The fresh feed follows a linear profile, maintaining a constant $\mathrm{d}F/\mathrm{d}t$ via the RAMP function, while the recycled feed follows a sinusoidal profile via SRAMP to approximate smooth acceleration of time-dependent changes. The RAMP and SRAMP functions command selected blocks (flow controllers) to change a process variable to a given setpoint over a specified duration. In this work, the fresh feed uses RAMP, which implements a linear trajectory (constant $\mathrm{d}F/\mathrm{d}t$), while the recycled feed uses SRAMP, which produces a smooth, sinusoidal-like transition to approximate gradual acceleration. Both ramps are executed in parallel inside a PARALLEL condition so that both commands are executed simultaneously.

An illustrative task configuration is given in listing 3.1, where the fresh feed and the recycled stream are ramped down from the initial steady state to 40.0 kmol/h and 216.0 kmol/h respectively over 30 minutes. The task is set to start at 10 min into the simulation, making it easier to identify the steady state before the ramping begins. SPRemote in the ramp functions indicates the flow controller blocks' set points are set remotely by this script, not by user specification in the block configuration window.

```
Task Rampdown Runs At 10.0
  PARALLEL
    RAMP(Blocks("FC-FRESH").SPRemote, 40.0, 30.0, CONTINUOUS);
    SRAMP(Blocks("FC-REC").SPRemote, 216.0, 30.0, CONTINUOUS);
  ENDPARALLEL
End
```

Listing 3.1: Example task configuration for ramping down reactor inlet streams.

The resulting simplified dynamic reactor model is illustrated in figure 3.4, showing the two inlet streams with their respective ramping profiles. The model is then used to evaluate system response under time-dependent inlet perturbations. The analysis focuses on key performance metrics including catalyst-bed temperature gradients, the potential for local hotspot formation, and stabilization times. These results define essential operability constraints and ensure that subsequent optimization respects the physical limitations of the plant.

3.2.2 Computational Methodology and Solver Configuration

When imported from Aspen Plus initially, although the reactor model is fully configured, it requires additional solver settings for the software to solve the system. In the "Solver Options" window, several modifications to the solver settings are made as follows. In the "Non Linear Solver" tab, Newton method is selected as the method with increased maximum divergent steps (50) and maximum iterations (250). In the "Integrator" tab, Implicit Euler method is selected with variable step size between 10^{-4} and 0.1, to ensure numerical accuracy while maintaining computational efficiency. The initial time step is set to 0.01. The dynamic reactor model employs a finite difference discretization

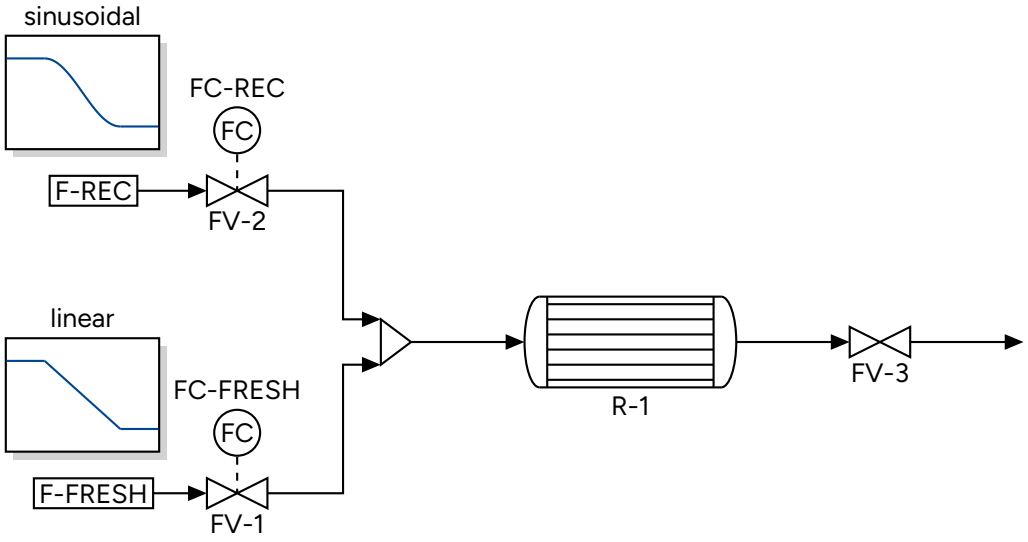

Figure 3.4: Simplified dynamic reactor model showing fresh and recycled feed streams with their control signal profiles.

scheme with 201 spatial nodes along the reactor length. This level of discretization balances the need for spatial resolution to capture temperature and concentration gradients with the computational demand of solving a large system of equations. Once converged, the model is initialized using steady-state conditions obtained from the Aspen Plus steady-state simulation, providing a consistent starting point for transient analysis.

3.2.3 Energy Balance

Aspen Plus Dynamics is an equation-oriented simulation environment, with model blocks written in a dialect of the programming language Modelica. By examining the equations implemented in the `RPlug` block, the energy-balance relationships solved by the software are identified. This review is necessary to interpret the available specifications when configuring the reactor model with overall heat-transfer coefficients.

The `RPlug` block calculates four distinct heat-exchange pairs: (i) between the coolant and the process stream, (ii) between the process stream and the reactor wall, (iii) between the process stream and the catalyst bed, and (iv) between the reactor tube wall and the environment.

This formulation is somewhat counterintuitive physically. The model first calculates overall duty between the process stream and the coolant via an internal heat-exchange submodel, and then separately evaluates heat transfer between the process stream and the wall and between the process stream and the catalyst. In effect, the implementation provides two parallel heat-removal pathways from the process stream—one directly to the coolant and one to the wall—rather than the serial pathway that exists in reality, where heat passes from process fluid to wall and subsequently from wall to coolant. In a rigorous transient model, the wall should act as an intermediate thermal mass,

capturing wall-temperature dynamics and thermal lag.

To address the physically inconsistent heat transfer simulation, the model is configured for this work to calculate the catalyst-bed temperature explicitly, while assuming that the reactor wall remains at the same temperature as the process stream and does not lose heat to the environment. This simplification removes the intermediate wall state and its associated dynamic lag, effectively collapsing the heat-transfer pathway into a single direct process-coolant resistance. Although this approach reduces computational complexity and avoids custom modifications to the implementation, neglecting the thermal mass of the reactor wall removes a thermal buffer that would otherwise dampen temperature fluctuations during transients. As a result, the simulated catalyst temperature differences during ramping are expected to be higher than those in a real reactor, where wall thermal inertia would attenuate the response. This limitation is discussed further in section 4.2.2 alongside the dynamic simulation results.

3.2.4 Minimum Load and Maximum Ramp Rates

The minimum operable load and maximum ramp rates are key parameters defining the reactor's flexibility. These constraints are informed by both literature recommendations and industrial practice, as well as the physical limitations of the catalyst and reactor design.

Minimum Load

The minimum operable load is determined differently in the literature. Nguyen [27] define the minimum load based on what Aspen Plus Dynamics can solve within reasonable computing time, whereas a subsequent publication fixes the minimum load at 20 % of nominal capacity to reflect mechanical constraints of reciprocating compressors [23]. Industrial perspectives suggest greater flexibility; for example, the FlexMethanol process by MAN Energy Solutions offers 10 and 20 MW modular skids (i.e., pre-assembled PtM units) that can each operate at loads from 10–100 % of nominal capacity [40]. In this work, the minimum load is set at 10 %.

Maximum Ramp Rates

In a methanol synthesis context, maximum ramp rates are typically constrained by allowable temporal change in catalyst temperature during transients. Heydorn and Diamond [41] recommend a maximum heating rate of 30 °C/h and a maximum cooling rate of −35 °C/h for their Liquid Phase Methanol (LPMeOH) process; Nguyen et al. [23] convert these to minute-based limits (0.50 °C/min and −0.583 °C/min). However, direct conversion from hourly averages to shorter timescales changes the physical interpretation: the instantaneous rate of change at some reactor position will always exceed the average slope over the full ramp. While Heydorn and Diamond [41] do not specify time resolution, very brief excursions (shorter than about 10 s) are unlikely to induce sintering or deactivation. Therefore, the maximum ramp rate in this work is evaluated from the average slope of the catalyst temperature over the ramp period,

$$\max_{z} \frac{\Delta T_{\text{cat}}(z)}{\Delta t} \tag{3.9}$$

and compared with the limits suggested by Heydorn and Diamond [41]. In addition, the instantaneous derivatives

$$\frac{\partial T_{\text{cat}}(z)}{\partial t} \tag{3.10}$$

are monitored to capture localized peaks in temperature-change rate during transients.

3.2.5 Reactor Specifications and Monitored Variables

The dynamic reactor model is configured with the specifications listed in table 3.6. The reactor employs a $Cu/ZnO/Al_2O_3$ catalyst with a bulk density of 1 750 kg/m^3 and void fraction of 0.275. The overall heat transfer coefficient between the coolant and the process stream is set to 118 W/(m^2 K).

Table 3.6: Dynamic reactor model specifications.

Parameter	**Value**	**Literature Reference**
Reactor length (m)	5.0	7.0 [24, 38]
Reactor tube diameter (m)	0.04	0.04 [22, 38]
Number of tubes	1 817	1 620 [38]; 1 340 [22]
Catalyst particle density (kg/m^3)	1 750	1 190 [38]; 1 775 [22]; 1 950 [24]
Bed void fraction	0.275	0.285 [38, 42]; 0.385 [24]
Particle diameter (mm)	3.65	5.4 [37]
Catalyst heat capacity (J/(kg K))	750	1 000 [24]
Overall heat transfer coeff. (W/(m^2 K))	118	118.4 [38]
Operating pressure (bar)	70	table 3.4
Inlet temperature (°C)	225	table 3.4

3.2.6 Steady-State Detection After Ramping

A straightforward analytical tool was created to determine the time required for the reactor to achieve steady-state conditions following completion of the ramping process. The steady-state detection method employs a two-part threshold system based on catalyst temperature derivatives over time. Once ramping concludes, steady-state conditions are verified when both criteria are met: (i) the root-mean-square (RMS) value of the temperature time derivative falls below the designated threshold, and (ii) the maximum absolute temperature change rate at any reactor location is less than 0.01 °C per minute:

$$\mathrm{RMS}\left(\frac{\partial T_{\mathrm{cat}}}{\partial t}\right) < 0.01\,^{\circ}\mathrm{C/min} \tag{3.11}$$

$$\max_{z}\left|\frac{\partial T_{\mathrm{cat}}(z)}{\partial t}\right| < 0.01\,^{\circ}\mathrm{C/min} \tag{3.12}$$

For each ramp experiment, the search for steady state is initiated once the ramp is completed. The first period in which both criteria are satisfied is designated as the onset of a new steady state.

3.3 MILP Optimization Model Formulation

3.3.1 Overview and Integration with Dynamic Modeling

The operational optimization of the e-methanol plant is formulated as a MILP problem that integrates physical limitations revealed by dynamic reactor simulations into an economically driven scheduling problem. The MILP formulation is necessary because the plant operates under a binary operational strategy with discrete capacity levels (100 % and 10 %), requiring integer decision variables to represent these on/off operational states. This naturally leads to a mixed-integer optimization problem where binary variables (0 or 1) represent the operational mode at each time period.

Historical electricity data from 2019 to 2023 in SE3 zone in Sweden is sourced from Nord Pool and fed to the model. These five years of data represent a wide range of market conditions, with different levels of average prices and volatility [43], providing a great range of scenarios to compare. Description and characterization of market conditions in relation to optimal operation is discussed in more detail in section 4.4.1.

An objective function is defined to maximize annual profit by balancing revenues from methanol sales against costs for electricity, CO_2 feedstock, variable operating expenses, and capital expenditures. It is assumed that captured CO_2 is locally available and purchased at a fixed price of EUR 80/t, reflecting current estimates for carbon capture costs from a large-scale process such as a combined heat and power (CHP) plant in Sweden [44]. The model is implemented in Python (v3.13) using Pyomo and solved with the commercial solver Gurobi.

By integrating dynamic modeling results with economic optimization, the economic assessment is now grounded in the physical constraints of the system, addressing both the engineering feasibility of flexible operation and its economic viability.

3.3.2 System Description and Configuration

The investigated e-methanol production system consists of two subsystems: an alkaline water electrolysis (AWE) unit for hydrogen production and a methanol synthesis plant constructed in section 3.1. AWE is selected for its technological maturity, lower capital cost compared to PEM

systems, and demonstrated capability for dynamic operation across a wide load range [21]. The electrolysis system capacity is designed to match the stoichiometric hydrogen demand from the methanol plant at its design capacity, ensuring full utilization of the hydrogen feedstock while accepting lower single-pass CO_2 conversion. The methanol synthesis plant operates at a design production rate determined by the feed flowrates specified in section 3.1.2.

The system is designed to operate under a binary operational strategy with two distinct modes to represent full-load and minimum-load operation. At full capacity, the plant consumes the total power required for both electrolysis and methanol plant auxiliaries, as determined from the steady-state process model. At minimum turndown, corresponding to the minimum load constraint established in section 3.2.4, total power consumption and methanol production decrease proportionally while maintaining process stability. The plant operates continuously at one of these two capacity levels and does not include a shutdown mode, reflecting the operational strategy validated through dynamic simulations.

3.3.3 Equipment Sizing and Economic Parameters

For economic evaluation of the plant, a preliminary "Class 4"[1] cost estimation is carried out for all equipment in the e-methanol production system. This level of estimation matches the process definition available from steady-state simulation and includes both the methanol synthesis process equipment and the alkaline water electrolysis system. While sizing unit operations in Aspen Plus is directly available using Aspen Process Economic Analyzer (APEA), the automatic mapping omits important details about key components such as the reactor and distillation column, rendering the results unreliable. Therefore, a cost-curve correlation method is employed using equation 3.13 and parameters extracted from Towler and Sinnott [45].

Methanol Plant Equipment Costing

The purchased equipment cost for methanol synthesis equipment is calculated using the standard correlation:

$$C_e = a + bS^n \tag{3.13}$$

where: C_e = purchased equipment cost in US dollars (reference CEPCI=532.9)
a, b = cost constants in table 3.7
S = size parameter, units, lower and upper bounds given in table 3.7
n = equipment type-specific exponent in table 3.7

[1] Following the Association for the Advancement of Cost Engineering (AACE) classification system, Class 4 estimates have a typical accuracy of ±30 % and are appropriate for preliminary feasibility studies based on limited cost data and design detail [45].

Table 3.7: Costing Constants for Methanol Plant Equipment [45].

Equipment	**Size parameter, S**	S_{lower}	S_{upper}	a	b	n
Reciprocating compressor 0	Power (kW)	93	16 800	260 000	2 700	0.75
U-tube S&T exchanger	Area (m²)	10	1 000	28 000	54	1.2
Floating head S&T exchanger	Area (m²)	10	1 000	32 000	70	1.2
Vertical pressure vessel	Shell mass (kg)	160	250 000	17 400	79	0.85
Sieve tray	Diameter (m)	0.5	5.0	130	440	1.8

From the process model built in Aspen Plus, key sizing parameters such as compressor power, heat exchanger area, vessel shell mass, and column diameter are extracted. All equipment costs are escalated from the base year (2010, CEPCI = 532.9) to 2025 values (CEPCI = 800). The purchased equipment cost calculated in USD is then converted to EUR using exchange rates for corresponding years. It is assumed that all equipment in direct contact with H_2 is constructed with stainless steel 316, while the rest is made of carbon steel. More detailed methods for cost estimation are provided in appendix B.

Electrolyzer System Costing

The AWE system is another component in the total capital investment and is costed separately from the methanol plant equipment. The electrolyzer cost correlation is based on its rated capacity, as given in equation 3.14:

$$C_{\text{electrolyzer}} = 1\,400 \times P_{\text{rated}} \tag{3.14}$$

where: $C_{\text{electrolyzer}}$ = electrolyzer purchase cost in EUR
P_{rated} = rated electrical capacity in kW
1 400 = specific cost in EUR/kW [46]

This specific cost is based on the Danish Energy Agency's technology catalogue, which reports 875–1400 EUR/kW for alkaline electrolyzer systems in the 10–100 MW range [46]. A value toward the upper end of this range is adopted, reflecting costs for systems below 100 MW scale. For comparison, the European Hydrogen Observatory reports higher values around 1666 EUR/kW based on 2023 market data, which includes full EPC costs [47]. The cost includes the complete electrolyzer stack, power electronics, gas processing equipment, and basic controls, but excludes balance-of-plant items such as water treatment and hydrogen compression, which are accounted for separately in the methanol plant auxiliaries.

The electrolyzer system is assumed to have a reduced installation factor compared to traditional chemical equipment, reflecting the modular nature of electrolyzer installations and the reduced civil

works requirements. The total installed electrolyzer cost represents the largest single equipment item in the integrated plant, as detailed in the economic analysis in chapter 4.

3.3.4 Mathematical Formulation

Objective Function

The MILP optimization model seeks to maximize annual economic profit over the planning horizon T by balancing revenues against all major cost components:

$$\max \quad \sum_{t \in T} \left[R_t - C_t^{\text{elec}} - C_t^{\text{CO}_2} - C_t^{\text{OPEX}} \right] - C^{\text{CAPEX}} - C^{\text{fixed}} \tag{3.15}$$

where: R_t = revenue from methanol sales
C_t^{elec} = electricity costs
$C_t^{\text{CO}_2}$ = CO_2 feedstock costs
C_t^{OPEX} = variable operating expenses
C^{CAPEX} = annualized capital expenditures
C^{fixed} = fixed operational costs

The electricity costs C_t^{elec} are calculated as the product of time-varying electricity prices and total system power consumption:

$$C_t^{\text{elec}} = \pi_{\text{elec}}[t] \times (P_{\text{electrolyzer}}[t] + P_{\text{process}}[t]) \tag{3.16}$$

where: $\pi_{\text{elec}}[t]$ = time-varying electricity price [EUR/MWh]
$P_{\text{electrolyzer}}[t]$ = electrolyzer power consumption [MW]
$P_{\text{process}}[t]$ = methanol synthesis process power consumption [MW]

Equation 3.15 represents the fundamental economic trade-off within the plant: maximizing methanol sales revenue while minimizing electricity purchases, CO_2 procurement, variable operations, and capital costs.

The economic performance of each operational strategy is evaluated using the levelized cost of methanol (LCoM), calculated as the total annualized costs divided by total methanol production:

$$\text{LCoM} = \frac{C^{\text{CAPEX}} + C^{\text{fixed}} + \sum_{t \in T} \left[C_t^{\text{elec}} + C_t^{\text{CO}_2} + C_t^{\text{OPEX}} \right]}{\sum_{t \in T} M_t} \tag{3.17}$$

where M_t represents methanol production rate at time t. This metric enables direct comparison between operational strategies by normalizing all costs to a per-tonne-of-methanol basis, accounting for both the total cost structure and production efficiency.

Decision Variables and Operational Constraints

The model employs binary decision variables to represent operational states:

$$x_{100}[t] \in \{0, 1\} \quad (100\,\% \text{ capacity operation}) \tag{3.18}$$
$$x_{10}[t] \in \{0, 1\} \quad (10\,\% \text{ capacity operation}) \tag{3.19}$$
$$y_{\text{up}}[t] \in \{0, 1\} \quad (\text{ramping up transition}) \tag{3.20}$$
$$y_{\text{down}}[t] \in \{0, 1\} \quad (\text{ramping down transition}) \tag{3.21}$$

The fundamental operational constraint ensures there is only one operational state per time period, i.e., either full load or minimum load:

$$x_{100}[t] + x_{10}[t] = 1 \quad \forall t \in T \tag{3.22}$$

Stabilization requirements prevent multiple ramping events within the stabilization period:

$$\sum_{\tau=t}^{t+T_{\text{min}}} (y_{\text{up}}[\tau] + y_{\text{down}}[\tau]) \leq 1 \quad \forall t \in T \tag{3.23}$$

where T_{min} represents the minimum time between consecutive ramping events. This constraint ensures that after any ramping event, no additional ramps can occur for the next 2 hours. The 2-hour minimum is a conservative choice that accounts for the hourly resolution of the MILP model and provides a margin for process stability. This constraint prevents excessive cycling by filtering out short-lived price fluctuations: for instance, a brief two-hour price spike would not justify a ramp-down followed immediately by a ramp-up..

Production rates and power consumption are defined as functions of operational states:

$$M_t = x_{100}[t]M_{100} + x_{10}[t]M_{10} + y_{\text{up}}[t]\frac{M_{10} + M_{100}}{2} + y_{\text{down}}[t]\frac{M_{100} + M_{10}}{2} \tag{3.24}$$
$$P_t = x_{100}[t]P_{100} + x_{10}[t]P_{10} + y_{\text{up}}[t]\frac{P_{10} + P_{100}}{2} + y_{\text{down}}[t]\frac{P_{100} + P_{10}}{2} \tag{3.25}$$

where: M_t = methanol production rate at time t
P_t = power consumption at time t
M_{100}, M_{10} = methanol production rates at 100 % and 10 % load
P_{100}, P_{10} = power consumption at 100 % and 10 % load

During ramping transitions, the plant operates at the average performance between the starting and ending operational states. When ramping up from minimum to maximum load, production rate and power consumption are calculated as the arithmetic mean of the two steady-state values. Similarly,

when ramping down from maximum to minimum load, the average values apply during the transition hour. This averaging reflects the physical reality that industrial processes transition gradually rather than instantaneously between operational setpoints.

The ramping transition approach ensures that the model accounts for the intermediate performance during load changes while maintaining computational tractability. The transition values are typically higher than the destination steady-state values, meaning that the optimization must balance the benefits of load changes against the operational characteristics during transitions.

3.3.5 Economic Assumptions

The economic evaluation of the e-methanol plant requires specification of cost parameters, pricing assumptions, and financial metrics that reflect realistic market conditions and industrial practice. The parameters are selected to represent current technology costs and market conditions and available literature values. The following paragraphs detail the major cost categories and pricing assumptions that are fed to the economic analysis.

Capital Expenditure Assumptions

Capital expenditure assumptions are based on current market data for alkaline electrolysis systems and established cost correlations for methanol plant equipment. The electrolyzer stack lifetime is set to 7.5 years and plant lifetime 25 years based on technical targets published by U.S. Department of Energy [35]. The methanol plant capital costs are annualized over the project lifetime (25 years) using a discount rate of 5 % to enable comparison with operational costs. Total annualized capital expenditures are calculated by combining both electrolysis and methanol synthesis equipment costs.

Operating Expenditure Assumptions

Operating expenditures are calculated as the sum of fixed and variable components, following standard industrial practice for chemical plant economic analysis [45]. Fixed operating expenditure (OPEX) comprises three main components: (1) methanol plant fixed operations and maintenance calculated as 4 % of the total installed equipment cost per year, (2) electrolyzer system fixed O&M (including personnel, routine maintenance, and insurance) calculated as EUR 43/kW per year [47], and (3) electrolyzer stack replacement costs amortized over the 7.5-year stack lifetime.

Variable OPEX scales with operational intensity and includes process utilities and performance-dependent maintenance. Electricity costs are excluded from variable OPEX and calculated separately to isolate the impact of dynamic operation under time-varying electricity prices, which is the central focus of this study. For the methanol synthesis plant, variable OPEX includes cooling water, steam, and other consumables required for continuous operation. For the electrolyzer, variable OPEX is effectively zero: the only consumable is demineralized water, whose cost contribution is negligible compared to electricity [48, 49]. During ramping transitions, variable OPEX is calculated as the

arithmetic mean between the starting and ending operational states to reflect intermediate performance levels.

Market Pricing Data

Historical hourly prices from Nord Pool SE3 zone[2] are used for the electricity pricing data. The optimization is performed separately for each calendar year (2019–2023), with each year's hourly price profile representing a distinct market scenario. Profitability metrics are then computed by combining each year's operational revenues and costs with the annualized CAPEX and fixed OPEX, which are independent of electricity prices and remain constant across scenarios. The methanol sales price is assumed to be EUR 850 per metric tonne, reflecting current market premiums for green methanol production in EU [50], accounting for the value proposition of renewable-based chemical synthesis. For comparison, conventional fossil-based methanol trades at approximately EUR 400 per tonne [51]. CO_2 purchase cost is assumed at 80 EUR/t, the cost-optimal value identified by Karlsson et al. [52] for Swedish CCS supply chains.

Table 3.8 summarizes all key economic parameters adopted in this study and compares them with representative values or ranges reported in the literature.

Table 3.8: Key economic parameters: adopted values and literature ranges.

Parameter	**This Study**	**Literature Reference**
Captured CO_2 cost (EUR/t)	80	35–174 [44]; 43–86 [53]
Methanol sales price (EUR/t)[a]	850	700–1 400 [53]
Discount rate (%)	5	-
O&M (methanol plant) (%)[b]	4	2–10 [45]
Alkaline electrolyzer		
CAPEX (EUR/kW)	1 400	875–1400 [46]; 1666 [47]
O&M (EUR/kW/y)	43	43 [47]; 50 [54]
Stack cost (EUR/kW)	300	242–388 [55]
Plant lifetime (y)	25	20–40 [35]
Stack lifetime (y)	7.5	7–10 [35]
Specific energy consumption (kW h/kg H_2)	52	48–55 [35]

[a] Current production cost levels of e-methanol.
[b] Percentage of total installed equipment cost per year.

3.3.6 Case Studies

Representative price scenarios are used to evaluate the economic implications of flexibility. The first scenario assumes constant full-load operation, which provides a baseline against which to measure the benefits of dynamic scheduling. Flexible scenarios allow the model to exploit hourly electricity-price

[2]Nord Pool is the Nordic power exchange; SE3 is Sweden's third bidding zone, covering the greater Stockholm region and central Sweden.

variation while respecting all physical constraints. Comparison of the two cases quantifies the value of flexibility in terms of both profitability and operating patterns.

3.3.7 Model Limitations and Scope

The analysis employs several simplifying assumptions that define the study's scope while maintaining methodological rigor. The model assumes perfect foresight of electricity prices over the optimization horizon, which is realistic for day-ahead operational planning since European electricity markets provide 24-hour price forecasts. This approach provides an upper bound for economic performance and is standard practice in energy systems optimization literature for establishing theoretical potential. The binary operational strategy (100 %/10 % capacity) excludes intermediate capacity levels to maintain optimization tractability while capturing the fundamental trade-off between operational flexibility and cost. This conservative approach likely underestimates the benefits of continuous capacity modulation, making the economic analysis conservative. Industrial chemical plants often operate in discrete modes due to equipment constraints, process stability requirements, and safety considerations, supporting the practical relevance of this assumption.

4 Results and Discussion

4.1 Steady-State e-methanol Process Model Results

The steady-state process model developed in Aspen Plus converged successfully under the design operating conditions outlined in section 3.1.2. The model achieves stable operation with design feed flowrates of 100 kmol/h CO_2 and 300 kmol/h H_2, corresponding to a stoichiometric ratio of 3:1 for methanol synthesis. The process demonstrates effective CO_2 utilization with a single-pass conversion of 15.7 % and an overall CO_2 conversion of 99.1 % when accounting for the recycle stream. The target purity of the methanol product is achieved at 99.85 % by weight. Table 4.1 summarizes the key performance indicators for the steady-state operation.

Table 4.1: Steady-state process performance metrics.

Parameter	**Value**	**Unit**
Single-pass CO_2 conversion	15.7	%
Overall CO_2 conversion	99.1	%
Recycle ratio	5.3	-
Methanol production rate	27.8	kt/year
Methanol purity	99.85	wt%

4.2 Dynamic Reactor Model Results

4.2.1 Ramping Cycle Analysis

Ramping cycling test results are presented in this section. To verify the feasibility of hourly operation of the process, 60-min ramping time is selected. The heating rate limits apply when ramping up to higher loads due to increased exothermic reaction activity, while the cooling rate limits apply when ramping down to lower loads as the reaction heat generation decreases.

Figure 4.1 shows the temperature derivative analysis over time. The red solid line represents the maximum heating rate (max $\partial T_{\text{cat}}/\partial t$) and the blue solid line shows the maximum cooling rate (min $\partial T_{\text{cat}}/\partial t$). The dashed vertical lines indicate the start and end of the ramping period as well as the time when the system reaches a new steady state after ramping.

When examining the instantaneous temperature derivatives, there are locations where the rate of temperature change exceeds the minute-based equivalent of Heydorn and Diamond [41]'s recommended

limits (30 °C/h for heating and −35 °C/h for cooling, corresponding to 0.5 °C/min and −0.583 °C/min respectively), especially around the start and end of each ramp. However, as discussed in section 3.2, these original limits were specified as hourly averages, and brief instantaneous excursions above these rates do not necessarily indicate thermal damage to the catalyst.

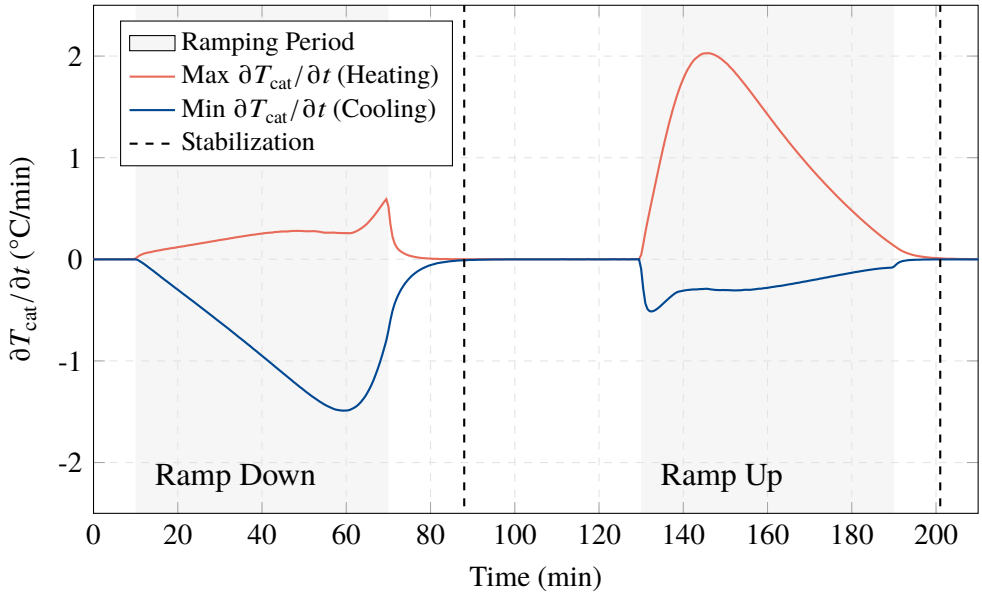

Figure 4.1: Temperature derivative analysis.

Figure 4.2 shows the average temperature change rate at each axial position in the catalytic bed during ramping. While the ramp-down curve remains within the acceptable range recommended by Heydorn and Diamond [41], the ramp-up curve slightly exceeds the upper limit of 30 °C/h near the reactor inlet, reaching approximately 35 °C/h. This exceedance is discussed further in section 4.2.2, where the conservative nature of the model is considered.

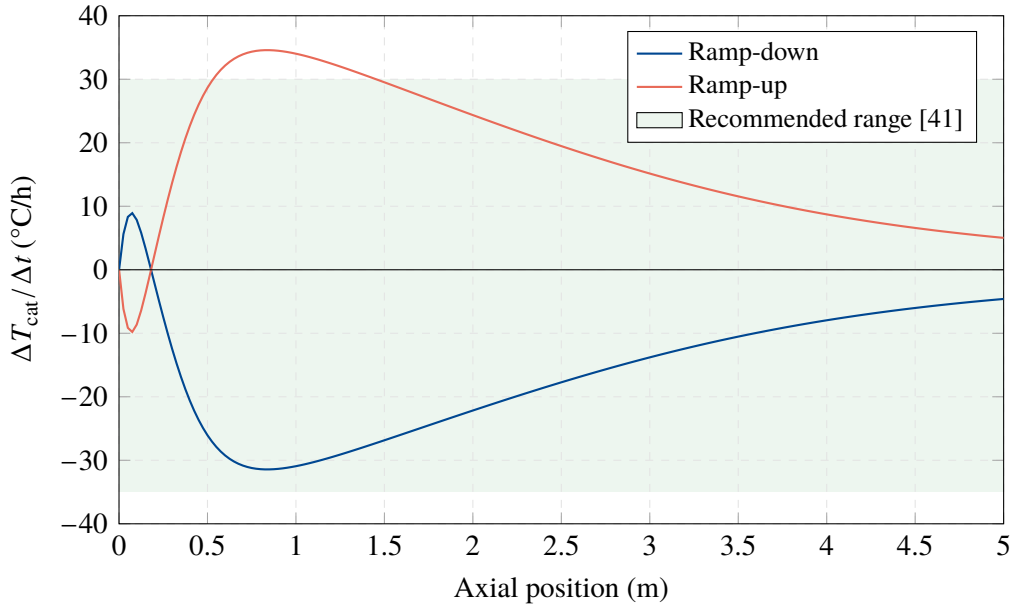

Figure 4.2: Ramping rate analysis along reactor axis.

Figure 4.3 shows the system reaches a new steady state around 10–18 minutes after ramping is finished. It is observed that it takes longer to reach a new steady state after ramping down compared to ramping up. This is likely due to the exothermic nature of the methanol synthesis reaction, which generates additional heat during operation at higher loads, thereby prolonging the stabilization period after a load decrease.

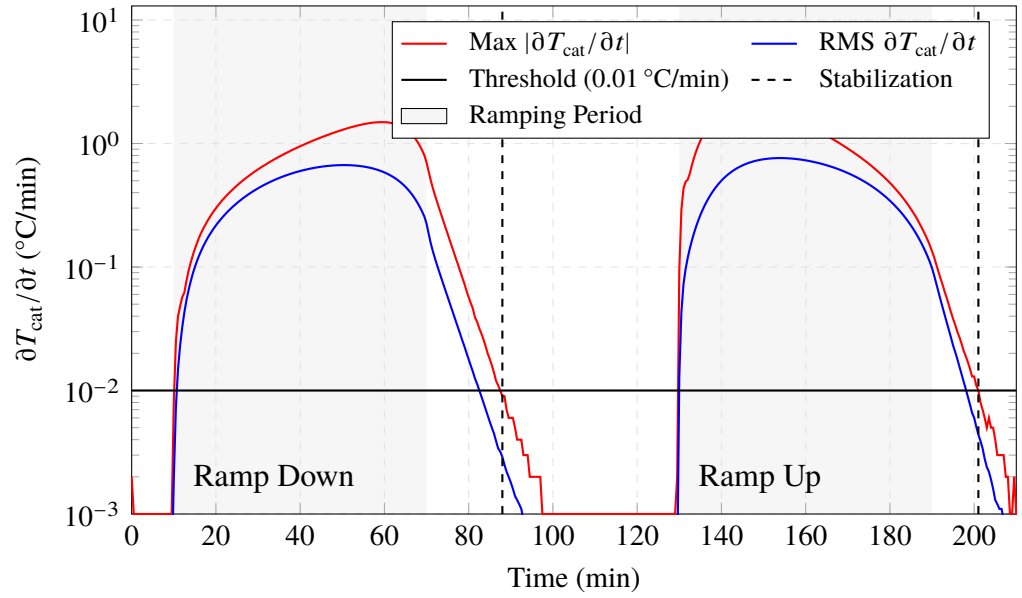

Figure 4.3: Stabilization criteria analysis.

Table 4.2 summarizes the key findings from the 60-minute ramping tests, including maximum and

average ramp rates, and stabilization time.

Table 4.2: Dynamic Reactor Analysis Summary (60-minute ramping)

Parameter	**Value**	**Units**
Data range	0 to 240	minutes (481 time steps)
Axial positions	201	points (0 to 5 meters)
Ramp-down start	10	minutes
Ramp-up start	130	minutes
First stabilization	88	minutes (after ramp-down)
Second stabilization	201	minutes (after ramp-up)
Ramp-down window	78	minutes (10 min → 88 min)
Ramp-up window	71	minutes (130 min → 201 min)

4.2.2 Dynamic Model Limitations: Energy Balance Simplification

As noted in section 3.2.3, the present dynamic reactor model assumes that the reactor wall remains at the same temperature as the process stream, effectively removing the wall as an intermediate thermal mass. This simplification has implications for the predicted temperature profiles during load-change scenarios.

In a physical reactor, the tube wall acts as a thermal buffer between the process fluid and the coolant. During ramp-up, the wall absorbs heat from the increasingly exothermic reaction before transferring it to the coolant, which dampens and delays the temperature response. Conversely, during ramp-down, the wall releases stored thermal energy, slowing the cooling of the catalyst bed. By omitting the thermal mass of the wall, the model predicts faster temperature responses than would occur in practice.

Consequently, the temperature change rates reported in figures 4.1 and 4.2 is likely overpredicted, as the thermal inertia of the wall would smooth out rapid transients. This explains why the ramp-up curve in figure 4.2 slightly exceeds the recommended limit: the actual reactor, with the wall acting as a thermal buffer, would experience lower peak heating rates. These effects are conservative from an operational planning perspective: if the simplified model indicates acceptable or only marginally exceeded thermal behavior, the actual reactor with additional thermal damping should perform within acceptable limits. Nevertheless, detailed experimental validation or higher-dimensional simulation including wall dynamics would be needed to confirm these predictions for final plant design.

4.3 Equipment Costing and Break-Even Analysis

Capital investment for the methanol synthesis process is estimated at 2.6 million EUR/y in annualized terms. This includes the reactor system, separation units, heat exchangers, and process control equipment required for methanol synthesis from captured CO_2 and electrolytic hydrogen. The cost

is based on the steady-state process model developed in section 3.1 and calculated using methods introduced in section 3.3.3.

As presented in table 3.8 in section 3.3.5, the electrolyzer cost was estimated with an assumed specific cost of 1 400 EUR/kW and 25-year economic lifetime. At the 31.4 MW design capacity, this translates to approximately 3.7 million EUR/y in annualized terms after amortization over 25 years. The electrolyzer sizing is based on the maximum hydrogen demand for full-capacity methanol production.

The combined annualized capital expenditure (CAPEX) (electrolyzer plus methanol plant) totals approximately 6.1 million EUR/y, representing 202 EUR/tonne of methanol at full annual production capacity. This annualization assumes a 25-year economic lifetime with a 5 % discount rate, following standard industrial practice for preliminary economic assessments.

4.3.1 Operational Expenditure Structure

The OPEX structure distinguishes between fixed costs that are independent of production level and variable costs that scale with operational intensity.

Fixed operational costs include maintenance, labor, insurance, and administrative expenses totaling 4 million EUR/y. This comprises:

- Methanol plant fixed O&M: 1.4 million EUR/y (4% of installed capital cost) [45]
- Electrolyzer fixed O&M (including stack replacement): 2.6 million EUR/y [54]

The fixed OPEX structure creates strong economic incentives for high capacity utilization, as these costs must be recovered regardless of production level.

Variable operational costs scale directly with production intensity and include process utilities excluding electricity. At full capacity operation, variable OPEX amounts to 85 EUR/h, while minimum-load operation at 10 % capacity incurs 25 EUR/h due to reduced throughput but similar auxiliary requirements.

4.3.2 Contribution Margin and Break-Even Electricity Price

The economic viability of hourly operation depends on the contribution margin, defined as the difference between revenue and variable costs:

$$\mathrm{CM}_t = R_{100} - \left(C_t^{\mathrm{el}} + C_t^{\mathrm{CO_2}} + C_t^{\mathrm{var}} \right) \tag{4.1}$$

where: R_{100} = hourly revenue from methanol sales at full capacity in EUR/h
C_t^{el} = hourly electricity cost in EUR/h
$C_t^{\mathrm{CO_2}}$ = hourly CO_2 cost in EUR/h
C_t^{var} = other variable operating costs in EUR/h

When the contribution margin is positive, each hour of full-capacity operation generates revenue that helps recover fixed costs. When the contribution margin is negative, continued operation incurs losses beyond the unavoidable fixed costs, and load reduction becomes economically favorable.

Since electricity cost is the only variable that changes hourly, setting CM = 0 and solving for electricity price yields the break-even electricity price:

$$\pi_{\text{breakeven}} = \frac{R_{100} - C_{100}^{\text{CO}_2} - C_{100}^{\text{var}}}{P_{100}} \tag{4.2}$$

where: $\pi_{\text{breakeven}}$ = break-even electricity price in EUR/MWh
$C_{100}^{\text{CO}_2}$ = CO_2 cost at full capacity in EUR/h
C_{100}^{var} = variable operating costs at full capacity in EUR/h
P_{100} = electricity consumption at full load in MW

The calculated break-even electricity price for 100 % load operation is 69.8 EUR/MWh. This threshold serves as the economic decision criterion: when hourly electricity prices fall below this value, full-capacity operation is optimal; when prices exceed it, load reduction minimizes losses.

The value of operational flexibility depends on market conditions. In a stable market with consistently high electricity prices and relatively low methanol prices, the contribution margin is frequently negative, and the ability to reduce load avoids accumulating losses during unfavorable hours. On the other hand, in a stable market with consistently low electricity prices, full-capacity operation yields positive contribution margins throughout the year, and flexibility provides little benefit. The greatest value emerges in volatile markets, where frequent price excursions above and below the break-even threshold create opportunities to avoid high-cost hours while capturing low-cost production periods.

4.4 MILP Optimization Results

Building on the cost structure and break-even threshold established in section 4.3, the MILP optimization model was solved independently for each calendar year from 2019 to 2023. Each single-year optimization uses the hourly electricity prices from that year to determine the profit-maximizing operational schedule, while annualized capital and fixed operating costs—amortized over the assumed 25-year plant lifetime—remain constant across all scenarios. This approach isolates the effect of electricity market conditions on operational strategy while maintaining consistent economic assumptions. One-hour ramping followed by one-hour of stabilization time is assumed based on the dynamic reactor analysis in section 4.2.

4.4.1 Operational Strategy Analysis

The optimized operational schedules reveal how the plant exploits market signals. Figure 4.4 presents a comprehensive overview of the optimization results for each year, showing electricity price patterns, breakeven thresholds, and the resulting operating mode selected in each hour.

Each subplot displays electricity prices sampled every 12 hours for visual clarity, while the optimization model uses hourly resolution. Operational zones are indicated by colored backgrounds: green areas represent periods of 100 % capacity operation, and yellow areas represent 10 % minimum load operation. The optimization model determines the most economical operational mode by comparing electricity costs to production revenues using the break-even electricity price threshold of 69.8 EUR/MWh.

The profiles reveal distinct patterns across different market conditions:

- **2019**: Stable, low-volatility conditions with predominantly full-capacity operation (99.0% utilization) and only occasional ramping events.
- **2020**: Similar stability with slightly lower average prices, prompting modest increases in minimum-load operation.
- **2021**: Moderate volatility introduces more frequent transitions between full load and minimum load as the plant arbitrages price swings.
- **2022**: Extreme volatility during the European energy crisis triggers frequent load adjustments and extended shutdown periods (47.5% utilization), reflecting aggressive demand-response behaviour.
- **2023**: Recovery-period pricing yields intermediate ramping frequency and improved operational stability compared to 2022.

These operating patterns provide context for the economic metrics analyzed in section 4.4.2.

4.4.2 Cost Comparison Across Years

Figure 4.5 compares LCoM for each strategy across the five-year analysis period. The dynamic optimization strategy reduces LCoM in most years, with the largest gains occurring during volatile market conditions.

In 2019, the optimization provides negligible LCoM reduction (0.2 EUR/t), as the stable, low-volatility market conditions offered few opportunities for price arbitrage. When electricity prices consistently remain low, the contribution margin is positive and the optimizer prefers full capacity operation almost every hour. With fixed costs dominating per-tonne costs, maximizing production volume is the most effective strategy; flexibility provides minimal benefit when there are few hours with negative contribution margins to avoid.

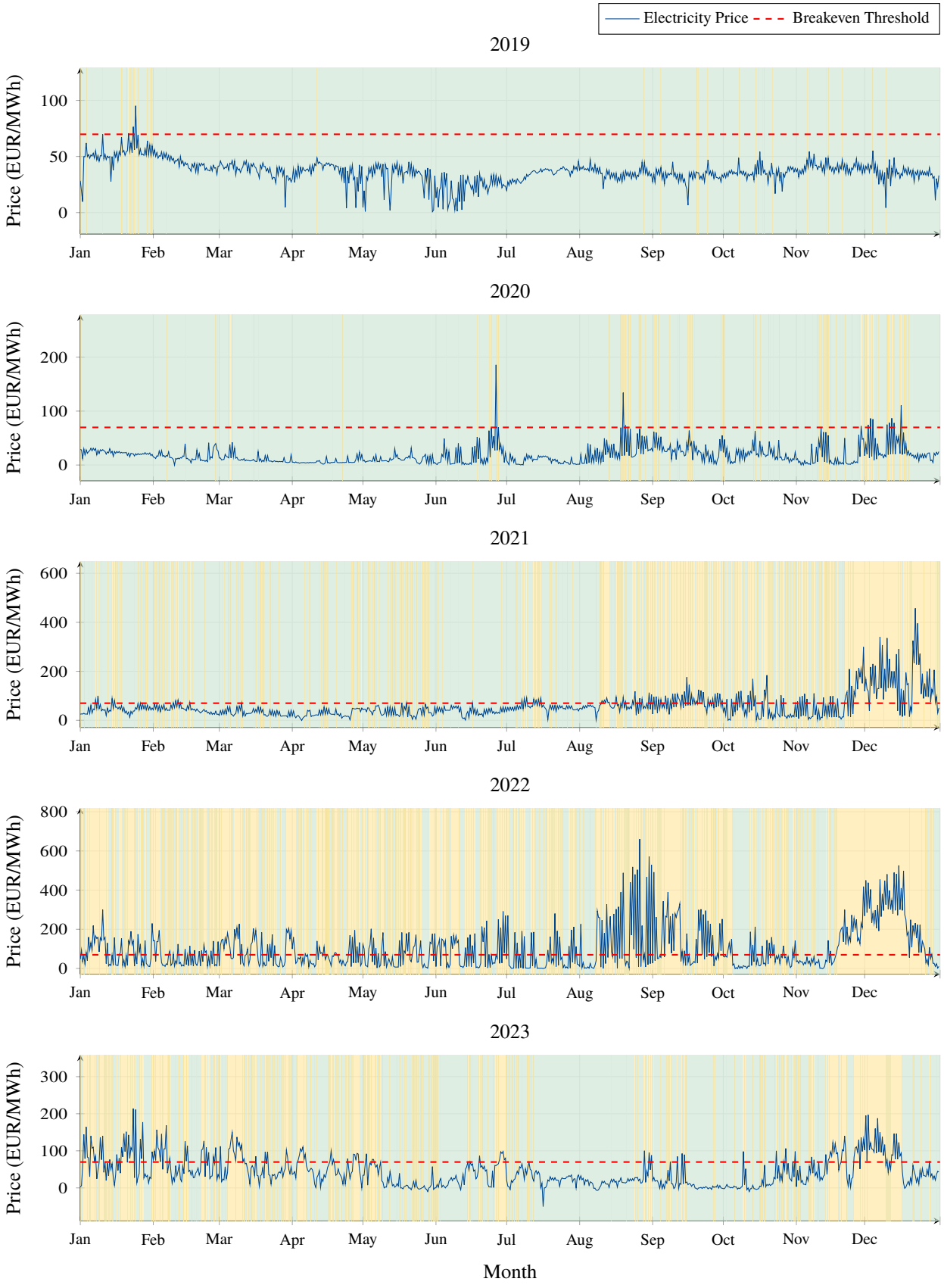

Figure 4.4: Multi-year operational profiles showing electricity prices (sampled every 12 hours) and optimal plant operation strategies (2019–2023).

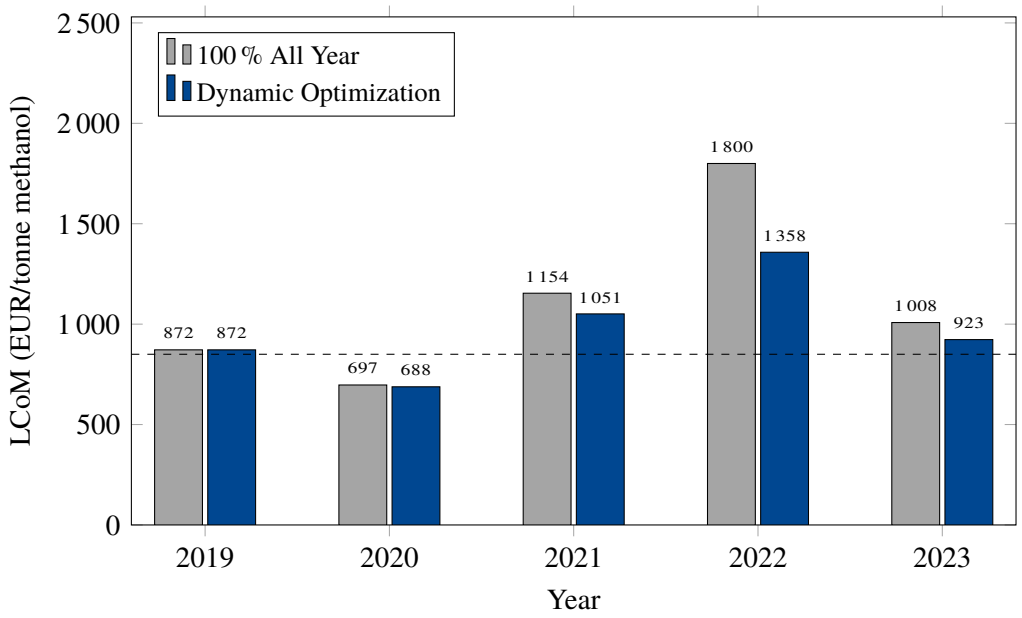

Figure 4.5: Multi-year cost comparison between fixed operation and dynamic optimization strategies.

- **2019**: 0.2 EUR/t savings (872.0 EUR/t → 871.8 EUR/t)
- **2020**: 8.6 EUR/t savings (696.6 EUR/t → 688.0 EUR/t)
- **2021**: 103.6 EUR/t savings (1 154.2 EUR/t → 1 050.6 EUR/t)
- **2022**: 441.0 EUR/t savings (1 799.5 EUR/t → 1 358.5 EUR/t)
- **2023**: 85.6 EUR/t savings (1 008.2 EUR/t → 922.6 EUR/t)

Volatile years (2021–2023) yield substantial LCoM reductions through flexibility, though in all scenarios the LCoM exceeds the assumed market price of e-methanol. Notably, 2020 was the only year where dynamic optimization achieved profitability, benefiting from both low average electricity prices and the ability to avoid the few high-price hours. This indicates that while operational flexibility captures significant value under volatile electricity markets, overall economic viability remains constrained by production costs.

4.4.3 LCoM Breakdown Analysis

The economic benefits of flexible operation are most prominent in years with high electricity price volatility. Figure 4.6 provides a detailed breakdown of LCoM for the year with the highest electricity prices (2022), comparing the 100 % all-year strategy with dynamic optimization.

The analysis reveals that electricity costs constitute the largest variable component, representing approximately 75 % of total costs in the 100 % strategy during 2022. Dynamic optimization reduces electricity costs by 770 EUR/t. The dramatic reduction in electricity costs (from 1 264 EUR/t to 494 EUR/t) more than compensates for the increases in per-unit fixed costs that result from reduced

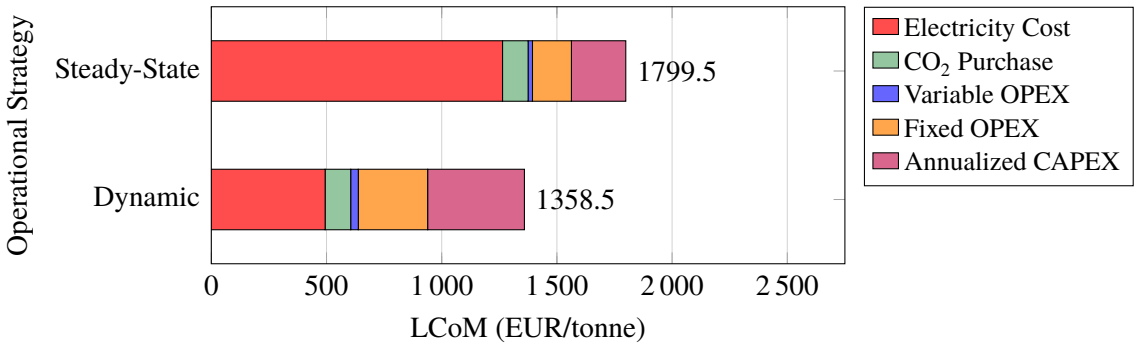

Figure 4.6: Cost breakdown comparison for 2022 showing the impact of dynamic operation on cost components.

plant utilization, though the decrease in the production volume leads to higher fixed costs per tonne of methanol produced.

4.5 Results Summary

This section provides a summary of the operational and economic performance across all analyzed years (2019–2023). The comprehensive analysis presented in table 4.3 summarizes insights about the quantified economic benefits as well as key metrics of dynamic e-methanol plant operation under varying electricity market conditions.

The economic benefits of operational flexibility demonstrate a strong correlation with electricity market volatility. Under the stable, low-price market conditions of 2019, dynamic optimization provided minimal cost difference, while the extreme volatility of 2022 enabled maximum savings of 441.0 EUR/t, representing a 24.5 % cost reduction compared to fixed operation.

The plant's operational profile adapts significantly to market conditions. Under the stable 2019 price scenario, the optimizer maintains full capacity for 99.0 % of the time with minimal ramping events (42 cycles). Conversely, under the volatile 2022 price scenario, the optimizer reduces full-load operation to only 47.5 % and requires 392 ramping cycles, exploiting price arbitrage opportunities.

The average cost savings across the five-year period amount to 128 EUR/t (12.9 % reduction), with individual yearly savings ranging from 0.2 EUR/t to 441.0 EUR/t. A strong correlation between electricity market conditions and the value of flexibility is confirmed.

Table 4.3: Comprehensive e-methanol Plant Operational Performance Analysis (2019–2023).

Metric	**2019**	**2020**	**2021**	**2022**	**2023**
Electricity market characteristics					
Market volatility	Low	Low	Medium	Very high	High
Actual year average (EUR/MWh)	38.4	21.2	66.0	129.2	51.7
Optimized avg. price (EUR/MWh)	38.0	19.3	43.0	47.6	30.3
Operational hours distribution					
100% load operation (hours)	8 659	8 476	6 118	3 654	6 091
10% load operation (hours)	101	284	2 642	5 106	2 669
Ramping transitions (hours)	85	253	641	785	589
Operational flexibility metrics					
Total ramping cycles[a]	42	126	320	392	294
Avg. 100 % period duration[b] (hours)	201.4	66.7	19.1	9.3	20.6
Avg. 10 % period duration[c] (hours)	2.3	2.2	8.2	13.0	9.0
Production performance					
Methanol production (tonnes/year)	27 512	26 989	20 254	13 216	20 177
Capacity utilization (%)	99.0	97.1	72.9	47.5	72.6
Economic performance					
100% all-year strategy LCoM (EUR/t)	872.0	696.6	1 154.2	1 799.5	1 008.2
Dynamic optimization LCoM (EUR/t)	871.8	688.0	1 050.6	1 358.5	922.6
Cost savings from flexibility (EUR/t)	0.2	8.6	103.6	441.0	85.6
Relative cost reduction (%)	0.0	1.2	9.0	24.5	8.5

[a] Number of complete load transitions (100 % → 10 % → 100 %) per year.
[b] Average duration of continuous full-load operation before ramping to minimum load.
[c] Average duration of continuous minimum-load operation before ramping to full load.

5 Conclusions

This study develops and validates a dynamic reactor model to characterize the thermal response and operational constraints of an e-methanol synthesis reactor under flexible operation. The primary contribution is establishing physically grounded ramp rates, stabilization times, and minimum load limits through dynamic simulation, which are then integrated into a year-scale MILP scheduling framework to assess the economic implications of flexibility under historical electricity-price volatility.

The main contributions are:

1. **Dynamic reactor modeling**: A detailed reactor model capturing catalyst bed temperature dynamics, reaction kinetics, and heat transfer limitations was developed and validated. 60-minute ramp tests established achievable ramp rates (100 % to 10 % capacity in one hour), stabilization times (10–18 min to reach steady-state thermal conditions), and operational constraints.
2. **Integrated optimization**: The validated operational boundaries (ramp rates, stabilization times, minimum load) were embedded into a parsimonious binary (100 %/10 %) MILP scheduling model. The binary representation is sufficient for the studied configuration where CO_2 supply tracks H_2 production; intermediate load levels would become relevant with independent CO_2 source constraints, minimum production commitments, or multi-unit plant designs.
3. **Multi-year economic assessment**: Using Nord Pool SE3 data (2019–2023), the optimization framework quantifies volatility-dependent economic gains from flexibility across stable and crisis market conditions, demonstrating how reactor-level constraints translate to system-level value.

Key Findings and Economic Insights

Flexibility value scales with price volatility: annual cost savings range from 0.2 to 441.0 EUR/tonne-methanol (0.0 to 24.5 % relative reduction) between 2019 and 2022. In the high-price 2022 baseline case electricity purchases account for about 80 % of total cost; dynamic operation lowers electricity cost by about 770 EUR/tonne-methanol (1 264 → 494 EUR/tonne) while maintaining product quality, partly offsetting higher specific fixed costs at reduced utilization.

Implications for Power-to-X Integration

Results indicate that the plant can both produce methanol and shift electrical load within validated ramp and stabilization limits, providing demand-side flexibility. A clear trade-off emerges: avoiding high-priced operation when variable costs exceed contribution margin versus underutilizing fixed investments when operating at minimum load. Future PtX system designs should treat flexibility (ramp rate, minimum load, response latency) as a first-order design variable rather than a downstream operational adjustment.

Future Market Context: The 15-Minute Resolution

The ongoing transition to a 15-minute Market Time Unit and imbalance settlement period across European electricity markets will quadruple the number of discrete price intervals relative to the hourly data used here, likely further increasing potential for flexible operation of PtX systems. The 60-minute ramps tested in this work would not capture sub-hourly price variations; achieving faster ramp capability and additional intermediate load levels could therefore unlock greater economic benefits than the hourly-resolution analysis quantifies here.

Limitations and Future Research Directions

This work has limitations that should be acknowledged while recognizing their conservative nature. In the dynamic modeling aspect, the analysis focuses only on the reactor, which contains the largest thermal mass and most complex kinetics, making it the primary bottleneck for dynamic response. This approach provides optimistic estimates of ramp times, since real plant response would likely be slower when considering heat integration effects.

The thermal rate limits used to verify ramp compliance are drawn from Heydorn and Diamond [41], which remains the only available quantitative source for dynamic thermal constraints in methanol synthesis; however, these limits were established for a liquid-phase slurry reactor, which differs from the conventional gas-phase fixed-bed configuration used in this work. The transferability of these limits to fixed-bed reactors is uncertain, and dedicated experimental or simulation studies on gas-phase reactor dynamics would strengthen the validity of the ramp rate verification.

In addition, only two operational states (100 % and 10 % capacity) were modeled to maintain optimization tractability while capturing the fundamental flexibility trade-offs; even more flexible operation modeling (e.g., with additional sustained intermediate load levels) might show even greater economic benefits. Catalyst degradation and electrolyzer stack aging effects affecting overall process efficiency are not explicitly linked to operational cycling frequency, which would be necessary for a more accurate long-term economic assessment accounting for equipment lifetime impacts. The economic model treats methanol and CO_2 prices as fixed, which is appropriate for establishing

upper-bound benefits and is consistent with standard practice in energy systems optimization studies. However, treating such prices as variables would enable even more strategic optimization.

Future research shall expand the scope in several directions. Multi-level load operation with intermediate capacity states would become relevant in systems with independent CO_2 source constraints, minimum production commitments, or multi-unit plant designs. Coupling degradation models to cycling intensity would provide more realistic long-term cost assessments. The transition to 15-minute electricity market settlement will create new arbitrage opportunities.

Bibliography

[1] REN21, "Renewables 2024 Global Status Report Collection," 2024.

[2] IRENA, "Renewable Capacity Statistics 2024," International Renewable Energy Agency, Abu Dhabi, 2024. ISBN: 978-92-9260-587-2.

[3] IRENA, "Renewable energy statistics 2025," International Renewable Energy Agency, Abu Dhabi, 2025. ISBN: 978-92-9260-675-6.

[4] S. Cevik and Y. Zhao, "Shocked: Electricity Price Volatility Spillovers in Europe," *IMF Working Papers*, vol. 2025, Jan. 10, 2025. DOI: 10.5089/9798400296901.001

[5] M. Pavlík, F. Kurimský, and K. Ševc, "Renewable Energy and Price Stability: An Analysis of Volatility and Market Shifts in the European Electricity Sector (2015–2025)," *Applied Sciences*, vol. 15, no. 12, p. 6397, Jan. 2025. DOI: 10.3390/app15126397

[6] N. P. Koirala et al., "Geopolitical risks and energy market dynamics," *Energy Economics*, vol. 150, p. 108 814, Oct. 2025. DOI: 10.1016/j.eneco.2025.108814

[7] K. Khan, "How do supply chain and geopolitical risks threaten energy security? A time and frequency analysis," *Energy*, vol. 316, p. 134 501, Feb. 1, 2025. DOI: 10.1016/j.energy.2025.134501

[8] European Commission. "Energy and the Green Deal," [Online]. Available: https://commission.europa.eu/topics/energy/energy-and-green-deal_en Accessed: Nov. 3, 2025.

[9] European Court of Auditors, "Review 01/2025: Making the EU electricity grid fit for net-zero emissions," European Court of Auditors, Apr. 2, 2025.

[10] J. Burre et al., "Power-to-X: Between Electricity Storage, e-Production, and Demand Side Management," *Chemie Ingenieur Technik*, vol. 92, no. 1–2, pp. 74–84, Nov. 28, 2019. DOI: 10.1002/cite.201900102

[11] G. Müller et al., "The costs of future energy technologies: A comprehensive review of power-to-X processes," *Journal of CO2 Utilization*, vol. 92, p. 103 019, Feb. 1, 2025. DOI: 10.1016/j.jcou.2025.103019

[12] C. Cunningham, "The Global Ammonia Market," Tabbre Research, London, 2024.

[13] AEA, "2024 Annual Report," Ammonia Energy Institution, 2024.

[14] A. Klerke et al., "Ammonia for hydrogen storage: Challenges and opportunities," *Journal of Materials Chemistry*, vol. 18, no. 20, p. 2304, 2008. DOI: 10.1039/b720020j

[15] S. Chatterjee, R. K. Parsapur, and K.-W. Huang, "Limitations of Ammonia as a Hydrogen Energy Carrier for the Transportation Sector," *ACS Energy Letters*, vol. 6, no. 12, pp. 4390–4394, 2021. DOI: 10.1021/acsenergylett.1c02189

[16] A. Tripodi, F. Conte, and I. Rossetti, "Carbon Dioxide Methanation: Design of a Fully Integrated Plant," *Energy & Fuels*, vol. 34, no. 6, pp. 7242–7256, Jun. 18, 2020. DOI: 10.1021/acs.energyfuels.0c00580

[17] B. C. Erdener et al., "A review of technical and regulatory limits for hydrogen blending in natural gas pipelines," *International Journal of Hydrogen Energy*, vol. 48, no. 14, pp. 5595–5617, Feb. 15, 2023. DOI: 10.1016/j.ijhydene.2022.10.254

[18] A. Lotfollahzade Moghaddam et al., "Methane pyrolysis for hydrogen production: Navigating the path to a net zero future," *Energy & Environmental Science*, vol. 18, no. 6, pp. 2747–2790, 2025. DOI: 10.1039/D4EE06191H

[19] Fortune Business Insights, "Methanol Market Size, Share & Industry Analysis," FBI101552, Sep. 22, 2025.

[20] M. Usman and T. Yamada, "Methanol Reforming for Hydrogen Production: Advances in Catalysts, Nanomaterials, Reactor Design, and Fuel Cell Integration," *ACS Engineering Au*, vol. 5, no. 4, pp. 314–346, Aug. 20, 2025. DOI: 10.1021/acsengineeringau.5c00031

[21] R. Cozzolino and G. Bella, "A review of electrolyzer-based systems providing grid ancillary services: Current status, market, challenges and future directions," *Frontiers in Energy Research*, vol. 12, Feb. 8, 2024. DOI: 10.3389/fenrg.2024.1358333

[22] S. Mbatha et al., "Detailed assessment of dynamic startup, shutdown, and flexibility of the adiabatic, gas-and water-cooled methanol fixed bed reactor: Comparison for power to methanol application," *Chemical Engineering Science*, vol. 319, p. 122 280, Jan. 2026. DOI: 10.1016/j.ces.2025.122280

[23] V. H. Nguyen, A. Laari, and T. Koiranen, "The effect of green hydrogen feed rate variations on e-methanol synthesis by dynamic simulation," *Chemical Engineering Research and Design*, vol. 212, pp. 293–306, Dec. 2024. DOI: 10.1016/j.cherd.2024.11.012

[24] X. Cui, S. K. Kær, and M. P. Nielsen, "Energy analysis and surrogate modeling for the green methanol production under dynamic operating conditions," *Fuel*, vol. 307, p. 121 924, Jan. 2022. DOI: 10.1016/j.fuel.2021.121924

[25] C. Chen and A. Yang, "Power-to-methanol: The role of process flexibility in the integration of variable renewable energy into chemical production," *Energy Conversion and Management*, vol. 228, p. 113 673, Jan. 2021. DOI: 10.1016/j.enconman.2020.113673

[26] R. Rinaldi and C. G. Visconti, "Flexible operations of a multi-tubular reactor for methanol synthesis from biogas exploiting green hydrogen," *Chemical Engineering Science*, vol. 272, p. 118 611, May 2023. DOI: 10.1016/j.ces.2023.118611

[27] V. H. Nguyen, "Dynamic Modeling of Methanol Synthesis from Electrolytic Hydrogen and Captured Carbon Dioxide," M.S. thesis, LUT University, 2022.

[28] A. Montebelli et al., "Optimization of compact multitubular fixed-bed reactors for the methanol synthesis loaded with highly conductive structured catalysts," *Chemical Engineering Journal*, vol. 255, pp. 257–265, Nov. 2014. DOI: 10.1016/j.cej.2014.06.050

[29] H. Sivert, "Flexibility in emerging e-methanol production in Sweden," M.S. thesis, Lund University, May 2024.

[30] S. Mucci, A. Mitsos, and D. Bongartz, "Cost-optimal Power-to-Methanol: Flexible operation or intermediate storage?" *Journal of Energy Storage*, vol. 72, p. 108 614, Nov. 2023. DOI: 10.1016/j.est.2023.108614

[31] E. C. Carlson, "Don't Gamble With Physical Properties For Simulations," *Chemical Engineering Progress*, Oct. 1996.

[32] K. M. Vanden Bussche and G. F. Froment, "A Steady-State Kinetic Model for Methanol Synthesis and the Water Gas Shift Reaction on a Commercial Cu/ZnO/Al2O3 Catalyst," *Journal of Catalysis*, vol. 161, no. 1, pp. 1–10, Jun. 1996. DOI: 10.1006/jcat.1996.0156

[33] J. Nyári et al., "Choice of the kinetic model significantly affects the outcome of techno-economic assessments of CO2-based methanol synthesis," *Energy Conversion and Management*, vol. 271, p. 116 200, Nov. 2022. DOI: 10.1016/j.enconman.2022.116200

[34] A. Rohatgi. "WebPlotDigitizer," WebPlotDigitizer, [Online]. Available: https://apps.automeris.io/wpd4/ Accessed: Sep. 9, 2025.

[35] U.S. Department of Energy. "Technical Targets for Liquid Alkaline Electrolysis," Energy.gov, [Online]. Available: https://www.energy.gov/eere/fuelcells/technical-targets-liquid-alkaline-electrolysis Accessed: Sep. 28, 2025.

[36] IMPCA, *IMPCA Methanol Reference Specifications*, version 10, Brussels, Sep. 10, 2024.

[37] F. Bisotti et al., "Impact of Kinetic Models on Methanol Synthesis Reactor Predictions: In Silico Assessment and Comparison with Industrial Data," *Industrial & Engineering Chemistry Research*, vol. 61, no. 5, pp. 2206–2226, Jan. 31, 2022. DOI: 10.1021/acs.iecr.1c04476

[38] L. Chen et al., "Optimization of Methanol Yield from a Lurgi Reactor," *Chemical Engineering & Technology*, vol. 34, no. 5, pp. 817–822, Mar. 21, 2011. DOI: 10.1002/ceat.201000282

[39] TMI Staff & Contributors. "Centrifugal vs reciprocating compressor," Turbo Machinery Magazine, [Online]. Available: https://www.turbomachinerymag.com/view/centrifugal-vs-reciprocating-compressor Accessed: Sep. 17, 2025.

[40] MAN Energy Solutions, *FlexMethanol: MAN DWE power-to-liquid (PtL) solutions*, 2023. [Online]. Available: https://www.man-es.com/docs/default-source/document-sync/flexmethanol-eng.pdf

[41] E. Heydorn and B. Diamond, "Commercial-Scale Demonstration of the Liquid Phase Methanol (LPMEOH) Process," *Final Report*, vol. 2, Jun. 2003.

[42] S. Mbatha et al., "Comparative evaluation of the power-to-methanol process configurations and assessment of process flexibility," *Energy Advances*, vol. 3, no. 9, pp. 2245–2270, 2024. DOI: 10.1039/D4YA00433G

[43] K. Marnate and S. Grönkvist, "Unlocking Sweden's hydrogen export potential: A Techno-Economic analysis of compressed hydrogen and chemical carriers," *Sustainable Energy Technologies and Assessments*, vol. 80, p. 104 359, Aug. 2025. DOI: 10.1016/j.seta.2025.104359

[44] S. Karlsson, F. Normann, and F. Johnsson, "Cost-optimal CO2 capture and transport infrastructure—A case study of Sweden," *International Journal of Greenhouse Gas Control*, vol. 132, p. 104 055, Feb. 2024. DOI: 10.1016/j.ijggc.2023.104055

[45] G. Towler and R. Sinnott, *Chemical Engineering Design: Principles, Practice and Economics of Plant and Process Design*. Elsevier, 2022, ISBN: 978-0-12-821179-3. DOI: 10.1016/B978-0-12-821179-3.00009-1

[46] Danish Energy Agency, "Technology Data – Renewable fuels," 2025.

[47] European Hydrogen Observatory, "The European hydrogen market landscape," European Hydrogen Observatory, Nov. 2024.

[48] A. Christensen, "Assessment of Hydrogen Production Costs from Electrolysis: United States and Europe," Jun. 18, 2020.

[49] W. Kuckshinrichs, T. Ketelaer, and J. C. Koj, "Economic Analysis of Improved Alkaline Water Electrolysis," *Frontiers in Energy Research*, vol. 5, Feb. 20, 2017. DOI: 10.3389/fenrg.2017.00001

[50] J. Dierickx, "Economic Value of Methanol for Shipping Under FuelEU Maritime and EU ETS," Methanol Institute, Methanol Institute, 2024.

[51] F. Schorn et al., "Methanol as a renewable energy carrier: An assessment of production and transportation costs for selected global locations," *Advances in Applied Energy*, vol. 3, p. 100 050, Aug. 25, 2021. DOI: 10.1016/j.adapen.2021.100050

[52] S. Karlsson et al., "Modeling the development of a carbon capture and transportation infrastructure for Swedish industry," *International Journal of Greenhouse Gas Control*, vol. 124, p. 103 840, Mar. 1, 2023. DOI: 10.1016/j.ijggc.2023.103840

[53] IRENA and Methanol Institute, "Innovation Outlook: Renewable Methanol," International Renewable Energy Agency, Abu Dhabi, 2021. ISBN: 978-92-9260-320-5.

[54] G. Glenk and S. Reichelstein, "Economics of converting renewable power to hydrogen," *Nature Energy*, vol. 4, no. 3, pp. 216–222, Mar. 2019. DOI: 10.1038/s41560-019-0326-1

[55] S. Krishnan et al., "Present and future cost of alkaline and PEM electrolyser stacks," *International Journal of Hydrogen Energy*, vol. 48, no. 83, pp. 32 313–32 330, Oct. 1, 2023. DOI: 10.1016/j.ijhydene.2023.05.031

A Aspen Plus Process Flowsheet

Figure A.1 shows the original process flowsheet as built in Aspen Plus V14. Figure 3.3 in section 3.1.2 is a reconstructed version of this flowsheet.

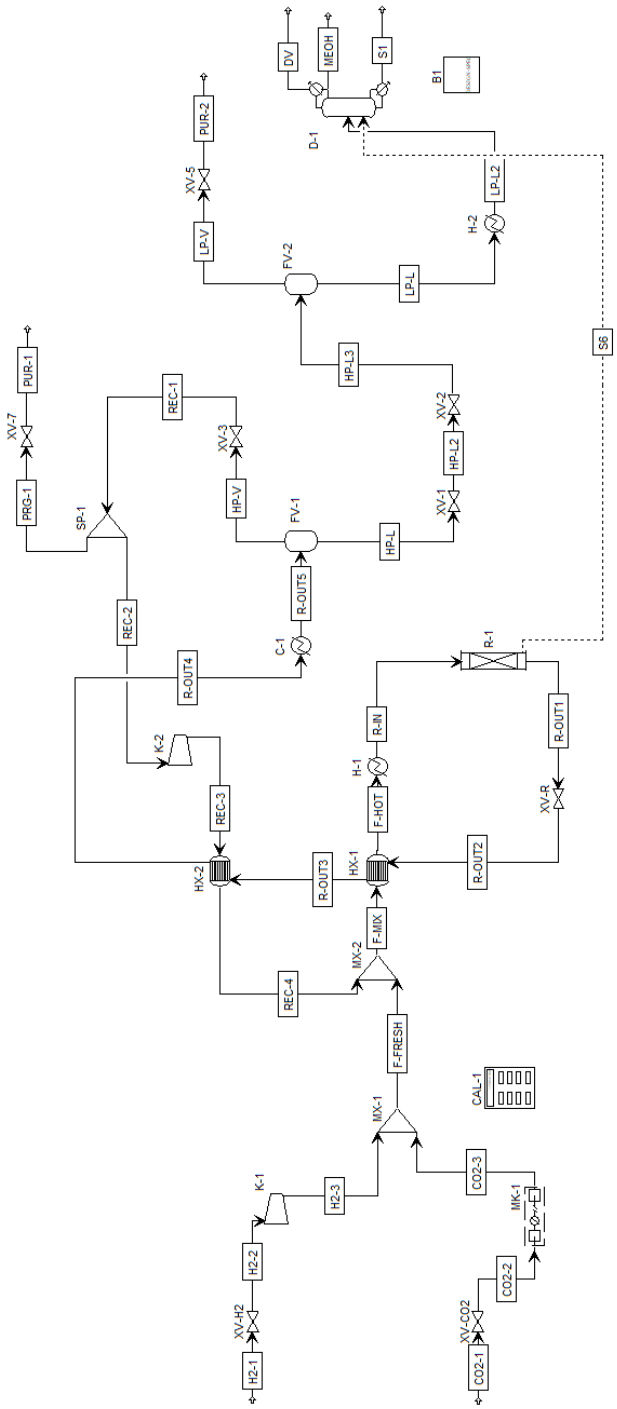

Figure A.1: Methanol synthesis process flowsheet in Aspen Plus V14.

B Cost Estimation Methodology

This appendix provides detailed information on the cost estimation methodology employed in this study, including cost index adjustments, currency conversion, material considerations, installed equipment cost calculations, and unit operation characterization for costing purposes.

Cost Index and Currency Adjustments

Equipment costs are adjusted using the Chemical Engineering Plant Cost Index (CEPCI) to account for inflation and temporal cost variations, and converted to EUR using annual average exchange rates.

Equation 3.13 and table 3.7 are based on US dollars with the base CEPCI in January 2010. Therefore, calculated costs are first adjusted to the current year using equation B.1, and then converted to EUR using equation B.2.

$$C_{\text{current}} = C_{\text{base}} \times \frac{\text{CEPCI}_{\text{current}}}{\text{CEPCI}_{\text{base}}} \tag{B.1}$$

$$C_{\text{EUR}} = C_{\text{USD}} \times \text{Exchange Rate}_{\text{USD/EUR}} \tag{B.2}$$

where: C_{current} = equipment cost in current year
C_{base} = equipment cost in base year
$\text{CEPCI}_{\text{current}}$ = cost index for current year
$\text{CEPCI}_{\text{base}}$ = cost index for base year
C_{EUR} = cost in EUR
C_{USD} = cost in US Dollars

The CEPCI values and USD/EUR exchange rates for the relevant years are presented in table B.1.

Table B.1: CEPCI values and USD/EUR exchange rates for cost adjustments (2019–2024).

Year	CEPCI	USD/EUR
2019	607.5	0.893
2020	596.2	0.876
2021	708.0	0.845
2022	816.0	0.950
2023	789.7	0.925
2024	824.2	0.908

Material Considerations

Material selection significantly impacts equipment costs due to varying material properties, availability, and processing requirements. This section outlines the material specifications and associated cost multipliers used in the economic evaluation.

Equipment material selection is based on process conditions, particularly:

- Operating pressure and temperature
- Fluid corrosivity (especially H_2 compatibility)
- Regulatory requirements for hydrogen service
- Economic considerations

Base equipment costs (carbon steel) are adjusted using material cost multipliers:

Table B.2: Material cost multipliers relative to carbon steel.

Material	**Multiplier**	**Application**
Carbon steel	1.0	Baseline material
Stainless steel 316	2.7	H_2 service, high corrosion resistance

Installed Equipment Cost Calculation

Purchased equipment costs are converted to installed costs using installation factors that account for:

- Direct installation labor
- Piping and instrumentation
- Electrical installation
- Insulation and painting
- Structural modifications
- Project management and engineering

The total installed cost is calculated using the factored cost method:

$$C_{\text{installed}} = C_{\text{purchased}} \times F_{\text{total}} \tag{B.3}$$

where: $C_{\text{installed}}$ = total installed equipment cost
$C_{\text{purchased}}$ = purchased equipment cost
F_{total} = total installation factor

Installation factors vary significantly by equipment type and complexity.

Table B.3: Installation factors for different equipment types.

Equipment Type	**Installation Factor**	**Complexity**
Reciprocating compressors	2.8	Medium
Shell-and-tube heat exchangers	3.2	Medium
Pressure vessels	4.1	Medium-High
Distillation columns	4.0	High
Packed-bed reactors	3.8	High

Pressure Vessel Mass Calculations

The mass of pressure vessels is calculated based on shell thickness and head geometry to determine material requirements for cost estimation. The minimum required vessel wall thickness t is computed using:

$$t = \frac{P_i D_i}{2SE - 1.2P_i} \tag{B.4}$$

where: t = vessel thickness
P_i = internal pressure
D_i = internal diameter
S = maximum allowable stress
E = welded joint efficiency

In this work, high-pressure vessels employ 2:1 American Society of Mechanical Engineers (ASME) ellipsoidal heads, while the low-pressure vessel (FV-2) uses torispherical heads for cost savings. A joint efficiency of 0.95 and a minimum wall thickness of 5 mm are assumed.

Unit Operation Characterization

The multi-tubular catalytic reactor consists of a tube-and-shell heat exchanger with catalyst packed in the tubes. The distillation column includes a shell-and-tube condenser, kettle reboiler, and sieve trays.